12-2020

Paleotectonic Investigation by Successive 3D Seismic Horizon Flattening in the Pennsylvanian Interval of Western Osage County, Oklahoma

Douglas Cooper McCabe
University of Arkansas, Fayetteville

Paleotectonic Investigation by Successive 3D Seismic Horizon Flattening in the Pennsylvanian Interval of Western Osage County, Oklahoma

A thesis submitted in partial fulfillment
of the requirements for the degree of
Master of Science in Geology

by

Douglas Cooper McCabe
Texas Tech University
Bachelor of Science in Geosciences with a
concentration in Geology, 2018

December 2020
University of Arkansas

This thesis is approved for recommendation to the Graduate Council

____
Christopher L. Liner, Ph.D.
Thesis Director

____
T. A. “Mac” McGilvery, Ph.D.
Committee Member

____
Gregory Dumond, Ph.D.
Committee Member

____
Steve Milligan, M.S.
Committee Member

Abstract

3D seismic and well log data in Western Osage County, Oklahoma, are utilized to evaluate possible intracratonic tectonic signals present in the subsurface stratigraphy of the Cherokee Platform as a result of the regional tectonic events of Pennsylvanian age. These events include: the Wichita, Ouachita, and Arbuckle orogenies, the Nemaha and Ozark Uplifts, and the Southeast Oklahoma Aulacogen. Horizon flattening within 3D seismic volumes allows for identification of paleotectonic structures and syntectonic depositional features, which may be related to the collateral effects of these orogenies on the Cherokee Platform. Identified structures were assigned geologic ages using precision synthetic seismograms tuned to the Pennsylvanian interval in a 45 square mile 3D seismic data volume. Paleostructure maps and isochron, or time-thickness, maps created in conjunction with the flattened horizons highlight contemporaneous structural features that may be related to regional orogenic events. Paleostructure maps also help determine the sedimentological processes occurring at the time of deposition. This investigation will add knowledge to the tectonic and depositional evolution of the Cherokee Platform and the surrounding basins, which have been prolific hydrocarbon-producing regions for over a century.

Acknowledgements

First and foremost, I want to thank my advisory committee: Dr. Chris Liner, Dr. Mac McGilvery, Mr. Steve Milligan, and Dr. Greg Dumond. These gentlemen led me through one of the most difficult jobs I have ever had to do, and we made it out on the other side—even if it meant they had to talk slower and repeat a lot. I owe these guys everything that I have accomplished and ever will accomplish in my life as a geoscientist. Thank you, Gents.

Next, of course is my family. DT, Anna, Parker, Cody, and Annie, if y'all hadn't worn me out asking "Is your thesis done yet?" I would probably be stretching it out another semester or two. All of you knew I could do it, even when I thought I couldn't. I guess that's what family is for.

To the Morvens: When COVID hit, you provided me a place to get some serious work done, and if you hadn't, I would definitely be rooting around in the weeds at this very moment. Pete, that workstation was bomber; Andrew, those two-a-days kept me fresh; and Ben, those breaks to watch golf and listen to music were the perfect punctuation marks on the days in that house/office. Neill, keep trolling, my man—even when I was flustered with this project, I got a good kick out of your random shots at just about everyone.

Finally, I would like to acknowledge that this project benefited from data and expertise provided to the Department of Geosciences by Shane Matson, Charles Wickstrom, Ron Snyder, and Don Unruh. Another, special thanks goes to the Osage Mineral Council, without whom I would not have had a project in the first place.

Thank You

Table of Contents

1. Introduction

1.1 Osage County History

Osage County, Oklahoma is located in the northeastern portion of the state of Oklahoma, Osage County (Figure 1). It is the largest county in the state (1.47 million acres) and has been owned by the Osage Indian Tribe since 1872 (Bass, 1942). Bordering Kansas to the north and five other Oklahoma counties to the west, south, and east. Osage County is also the key geographic area that defines the Cherokee Platform geologic province of Oklahoma as part of the Mid-Continent geologic region of the United States. Since the late 19^{th} Century, Osage County, Oklahoma (Figure 1) has been one of the most prolific oil and gas producing counties in the United States. When oil was first discovered in Osage County in 1897 (after earlier drilling efforts in 1896), production of petroleum products became the dominant economic activity in the county, garnering upwards of $279 million of income for the Osage Tribe by June 30, 1940 (Bass, 1942). Because of the success of the hydrocarbon fields in Osage County, there have been many exploration efforts in the time since the Bass (1942) reports were published. These efforts have produced many datasets to draw from, most notably the 3D seismic surveys and the well logs that were used in this thesis project.

The oil and gas producing zones of the Osage County subsurface are in Ordovician, Mississippian, and Pennsylvanian intervals with the main producers coming from Pennsylvanian aged rocks. New efforts to develop plays in the Mississippian interval, specifically the Mississippi Chat, are currently underway, but this project focuses on the Pennsylvanian units in the subsurface of Osage County.

Osage County is surrounded by geologic regions (Figure 1) that resulted from large-scale tectonic activity, particularly during the Pennsylvanian period. It is well established that the geology of Osage County is a part of the tectonically stable Cherokee Platform. The question is, are there subtle structural effects within the Cherokee Platform that are related to the larger, flanking events? It is hypothesized that there have been small tectonic influences on the Cherokee Platform, and it is the goal of this investigation to identify and characterize those signals.

1.2 Study Area and Data

The western portion of Osage County is characterized by Pennsylvanian-aged outcrops as well as Mississippian and Pennsylvanian-aged subsurface strata. Three 3D seismic surveys that encompass a cumulative 139 square miles are used in this investigation, labeled as WC, GH and AN on Figure 3. The seismic survey data were acquired in 1995-1996 and are used courtesy of the Osage Nation Minerals council. Acquisition parameters for each of the surveys are outlined in Table 1. One well in survey WC, which is referred to as "Well A" due to its proprietary nature, was also used in this investigation. Well A has a modern log suite including gamma ray, sonic, and electric logs, which allow for generation of a synthetic seismogram in order to accurately tie geologic well tops to seismic reflection events at the well location. Figure 4 exhibits a synthetic seismogram generated using OpendTect (dGB Earth Sciences, 2020) for Well A in WC (C. Liner, personal comm.). A time-depth conversion curve was also derived from Well A (Figure 5). The time-depth curve is used to convert two-way travel time to measured depth within the confines of the survey.

2. Geologic Setting

Osage County, Oklahoma lies within the Cherokee Platform geologic province that is bounded by the Nemaha Ridge to the west, the Ozark Uplift to the east, the Anadarko basin to the south, and farther south the Ouachita, Arbuckle, and Wichita Uplifts (Figures 1 and 6). Sea level variations and tectonic uplift/subsidence caused periods of seaway extension from southeast to northwest across modern day Osage County, allowing deposition of a mixture of marine and river delta sandstones, limestones, and shales in the Arkoma Basin to the southeast of Osage County and on the Cherokee Platform (Thorman et al., 1979).

The stratigraphic framework of the Pennsylvanian interval (Figure 2), as mentioned previously, is chiefly comprised of sandstones, limestones, and shales. Of the Desmoinesian groups—the Cherokee and Marmaton groups—the Cherokee Group is larger and is comprised of six sandstone units (three of which are prolific petroleum producers) and three limestone units (Liner et al., 2013). The Marmaton Group is comprised of two limestone units, one shale unit, and a sandstone unit (Liner et al., 2013). The Missourian series is comprised of two main groups, the Skiatook and Ochelata Groups, and the upper portion of the Marmaton Group (Liner et al., 2013). These groups are made of mainly sandstones with limestone units interbedded within the sandstones (Liner et al., 2013). Finally, the Virgillian-aged groups, the Douglas, Shawnee, and Wabaunsee Groups are also comprised of mainly sandstones with limestones emplaced within the sandstone units. It is important to note that the Cherokee Platform of Osage County is missing two key series: Morrowan and Atokan. This can present some difficulty when attempting to designate a hard timeline of structural deformation.

3. Tectonic History

The tectonic history of the Cherokee Platform is relatively uneventful when compared to the surrounding geologic provinces as seen in Figures 1 and 6. However, the impacts upon the Cherokee Platform from the surrounding tectonic provinces are important to consider when evaluating the depositional history of sediments on the Cherokee Platform. The tectonic boundaries of the Cherokee Platform geological province are the Nemaha Ridge to the west, the

Ozark Uplift (a product of the Ouachita Orogeny) to the east, the Ouachita and Arbuckle Uplifts, and the Anadarko Basin to the southeast, south, and southwest, respectively. The timing of these events is not precisely agreed upon but influenced the timing and style of deposition on the Cherokee Platform and the surrounding basins. It is therefore important to ascribe proper ages for these tectonic events as accurately as possible. A brief history of each of the previously mentioned tectonic events will be provided.

3.1 The Ouachita Orogeny

The Ouachita Orogeny extends in a general E-W trend from the southern portion of Arkansas, through southern Oklahoma, and into the Marathon region of Texas (Figure 6). Many contend that this orogenic belt is a composite of the Appalachian system and is a precursor for the Ancestral Rockies. The Ouachita Orogeny has been the source of contention between researchers with regards to the timing of its genesis. Houseknecht and Kacena (1983), Houseknecht (1986), and others postulate that the subduction zone was not initiated until the latest Devonian or earliest Mississippian time. Houseknecht's 1986 model is used here to orient the reader (Figure 7).

The first tectonic phase of the Ouachita orogeny began during the late Precambrian to early Paleozoic with the rifting of the supercontinent Rodinia into Laurasia and Gondwana. This rifting phase initiated the development of an oceanic basin between Laurasia and Gondwana and an accompanying Atlantic-style continental margin on the southern edge of Laurasia (Figure 8) (Houseknecht, 1986).

The southern margin of Laurasia remained passive from the Cambrian until the late Devonian. Sedimentation into the adjacent Ouachita Trough would later become the Ouachita accretionary prism. A transition from a passive to active tectonic margin began during the late

Devonian and into the earliest Mississippian as the southward subduction of Laurasia beneath Llanoria initiated the closure of the deep oceanic basin and formed the Ouachita trough (Figure 7). The sediments deposited in the former deep basin were incorporated in the Ouachita accretionary prism associated with the activated subduction zone. This accretionary prism continued to develop throughout the Mississippian into the early Atokan (Figures 8 and 9) and was the primitive structural character of what would become the Ouachita Mountains. Houseknecht (1986) suggests that the precise timing of the activation of the subduction event is difficult to determine, but it is apparent that subduction was in progress during the earliest Mississippian based on orogenic and volcanic detritus present in the Stanley Formation in the Ouachita Mountains.

The combination of subduction slab-pull and vertical loading caused flexural bending in the southern margin of Laurasia, which culminated in widespread normal faulting in the foreland of the system during the Atokan (Figure 7). The dominant faulting style shifted from normal to foreland-style thrusting from late Atokan to Desmoinesian. The resultant uplift along the frontal thrust created an "orogenic welt" that would further develop into the Ouachita Mountains (Figure 7 and 9) (Houseknecht, 1986). Later, in the middle Pennsylvanian the core of the accretionary prism was breached, and the Ouachita Mountains moved into their adolescence as the subduction rate began to subside (Keller and Cebull, 1973). From the late Pennsylvanian into the Permian subduction and tectonism ceased. It is important to note that during this process, the Ozark Platform was deformed and slightly uplifted (almost like an intracratonic bulge) into the structure seen today, the Ozark Dome (McGilvery et al., 2016). The Ozark Dome is the easternmost boundary of the Cherokee Platform.

3.2 The Wichita and Arbuckle Uplifts

To the south of the Cherokee Platform sit the Wichita and Arbuckle Mountains (Figures 1 and 6). The Anadarko Basin, which is west-southwest of the Cherokee Platform, is also a product of the Wichita and Arbuckle tectonism. Prior to the onset of the Wichita Uplift, the Southern Oklahoma Aulacogen developed to the northeast of the uplift (Perry, 1988). The development of the Wichita Uplift began in the Chesterian (late Mississippian) and continued through the early Atokan (Algeo, 1992). During this interval, existing normal faults from the previous failed rifting were reactivated as moderately to steeply dipping reverse faults under compressional forces exerted by the Ouachita-Marathon Orogeny. These faults generally dip to the southwest, indicating NE-SW compression (Algeo, 1992; Perry, 1988). The foreland thrusting resulted in intense folding and faulting along the frontal belt and deposition of synorogenic arkosic sandstones into the Anadarko Basin (Algeo, 1992).

The culmination of the tectonic events of southern Oklahoma began in the middle-late Pennsylvanian (Virgilian) with the evolution of the Arbuckle Orogeny (Figures 1 and 6), which is a peripheral tectonic event of the Wichita Uplift. It is assumed that deformation of the Arbuckle Uplift was completed by the late Virgilian to the earliest Permian (Algeo, 1992; Perry, 1988). The Arbuckle Fault forms a northern structural domain boundary of a regional transpressional system. Wrench-fault tectonism is thought to have had an impact on the Arbuckle Uplift as well—an example of the type of continental wrenching seen in the Arbuckle Anticline is presented in a deformational model of the Western Arbuckles as described by Perry, 1988 as it is a complex sequence within a relatively short time interval:

> (1) Compression trending N. 35°-60° E., associated with the Arbuckle thrust of Brown (1984), produced mesoscopic folds and contraction faults on the northeast limb of the Arbuckle anticline in

> the Lake Classen area. (2) These mesoscopic structures were then rotated to or past the vertical within enveloping Ordovician to Mississippian strata. (3) Several kilometers of erosion occurred such that the inferred Ada-equivalent (middle Virgilian) Collings Ranch Conglomerate rests on steeply dipping Ordovician rocks. Phases 1, 2, and 3 may have closely overlapped in time. Left-reverse slip on the Arbuckle thrust north of the Arbuckle anticline is indicated by en echelon anticlines and synclines on the hanging wall of this thrust… (4) About 4.3 km (2.7 mi) of left slip developed on the Washita Valley fault… The array of very Late Pennsylvanian strike-slip faults in this area indicates that the compression direction had rotated to about N. 70°-75° E. during final phases of deformation.

The tectonic history of the Arbuckle Uplift lends credence to the transpressional system hypothesis of the Ouachita system. The Wichita and Arbuckle Uplifts are hypothesized to have impacted the geologic structure of the Cherokee Platform in the Missourian due to their proximity and magnitude of deformation (Barker, 2018).

3.3 The Nemaha Ridge

The Nemaha uplift (Figures 1 and 6) developed perpendicular to the general strike of the Ouachita system via E-W compressional thrusting and strike-slip deformation, displaying a general southern structural plunge (Dolton and Finn, 1989; Gay, 2003; Snyder, 1968). This occurred during the early Pennsylvanian into the early Permian (Dolton and Finn, 1989). The Nemaha Ridge trends from its northern limit in Kansas and Nebraska to its southern limit in northern Oklahoma and is the westernmost geographical limit of the Cherokee Platform. The Nemaha displays v-shaped pop-up blocks in the subsurface in Oklahoma, and it was first recognized as a hydrocarbon exploration target in Oklahoma in the early 20th century (Gay, 2003). Since the time of its discovery, there have been many hypotheses describing the origin of the Nemaha Uplift, but most contemporary models such as Gay (2003) posit that compressional and strike-slip processes shaped its current structure, explaining the thrusting, folding, and lateral displacement observed.

4. Previous Investigations

No previous publications describe the use of 3D seismic horizon flattening techniques in conjunction with isochron mapping to highlight tectonic signals in a stable cratonic setting. . Horizon flattening, however, is a widely used method of seismic interpretation to estimate paleodepositional settings by restoring original horizontality to the horizon that is flattened. This allows investigators to interpret depositional trends and systems seen above and below the flattened horizon.

There have been previous investigations in this study area by many researchers with a wide variety of goals using the same or very similar data sets to be used in this investigation. Benson (2014) and Falzone (pers. Comm) deal directly with the mapping of Mississippian tripolitic chert bodies and the Mississippi Chat lithofacies in western Osage County. Investigation of deep basement seismic features in Osage County has been conducted by Liner (2015), and subsurface mapping and characterization of clinoforms in the Pennsylvanian interval can be found in Barker (2018). There have also been publications on the subsurface sequence stratigraphy of the Pennsylvanian interval by West (2015), the mechanical stratigraphy of the Mississippian intervals by Jennings (2014), and the stratigraphy and reservoir implications of the Arbuckle Group done by Keeling (2016)—all of which were done in western Osage County. West (2015) and Barker (2018) are of particular importance as the clinoforms that they investigated play a major role in this investigation. Other research conducted in this geologic region include Chenoweth (1968), Suriamin and Pranter (2018), Wittman (2013), Roy et al. (2012), Elebiju et al. (2011), and Clinton (1957).

Many theses and research articles have been completed regarding the structural development of the Arkoma Basin, Anadarko Basin, the Ouachita Orogeny (most of which include the development of the Ozark Dome as a product of the Ouachita Orogeny), Wichita and Arbuckle Uplifts, the Nemaha Ridge, some of which have been detailed in the previous section.

5. Methods

5.1 Data Analysis

The bulk of this investigation was conducted within the confines of the WC 3D seismic survey. This is the survey with the most previous work, and it provides a higher resolution dataset than surveys GH and AN. High resolution seismic horizons within the Pennsylvanian interval in the 3D seismic surveys were tracked, named, and catalogued. Horizon naming was determined by the well tops that are tied into WC using a synthetic seismogram based on well A sonic and density logs and an extracted wavelet tuned to the Pennsylvanian interval. For horizons that do not correlate with a known formation top in Well A, a name was given based on its time-depth in milliseconds on that synthetic; for example, horizon “264” was picked on a reflector that represents a two-way travel time of 264 ms. Once these horizons were tracked and catalogued, the flattening process began. First, the horizons were gridded and flattened. The flattened horizons were subsequently examined for any tectonic signals that might be present above or below the flattened horizon. This process gave insight into intracratonic activity within the Cherokee Platform as well as depositional constraints that may have been introduced as a result of this activity. These features are highlighted and catalogued as part of this study.

After cataloging probable tectonic signals, tracked horizons were used to create interval time maps. If regional tectonic forces warped the paleo-depositional surface up or down, it would result in thinning or thickening as the interval filled the new accommodation space. There are circumstances in which erosional surfaces can play a role in the outcome of the character of the isochron maps. This can be seen in this investigation on maps that are affected by the Mississippian-Pennsylvanian Unconformity. Interval analysis allows a more accurate timing estimate of the tectonic signal, connection to surrounding tectonic systems, determination of orientation and sense of the signal (compressional or tensional), association with orogenic province, and serves as a proxy for paleo-geomorphology in a narrow band of geologic time. Isochron (time-thickness) maps were also constructed in selected intervals to evaluate sediment dispersal. These time-thickness maps were constructed using the composite tectonostratigraphic intervals. These intervals are TSI-1, TSI-2, TSI-3, and TSI-4. Isolation of the individual horizon pairs within each tectonostratigraphic sequence was used to illustrate large-scale time-thickness and small-scale time-thickness, respectively. The naming convention for the isochron maps is derived from the process of constructing the isochron maps themselves. For each of the internal horizon pair maps, the name is a combination—in stratigraphic sequence—of the two horizons that comprise the interval of the map, e.g. the map that illustrates the time-thickness of the interval between the Osage/Layton horizon and the Avant horizon is called "Osage/Layton-Avant". Each horizon was gridded on a surface with a 3x3 smoothing filter to accurately interpolate time-structure between manually picked lines and to smooth tracking noise in the time-structure grid of the 3D autotracked horizons. Each interval is bounded by a basal and upper tracked horizon and isochron maps were constructed by subtracting the time-structure of the basal surface from the upper surface. This, in turn, gives the interval time-thickness—this is similar to the concept on an isopach map, but instead of using true stratigraphic thickness, the thicknesses being represented are derived from vertical two-way travel times present in the 3D seismic surveys.

The tectonic impact on depositional processes can be inferred from paleostructure and isochron maps. Based on the vectors associated with the features seen on the isochron maps, it can be determined from which tectonic event each signal is originating.

It is important for the reader to have a basic understanding of what kind of features were of interest in the interval time isopachs. Some of these are the long wavelength features that are being interpreted as tectonic signals for this investigation. The signals include, but are not limited to, clinoforms, stratigraphic thickening, stratigraphic thinning, stratigraphic truncations and pinchouts. The term 'long wavelength' is always relative to some reference length. In this study, features with length scales up to about half of the maximum survey dimension of 10 miles would be mappable and longer wavelength features would not. For example, a thickening ridge-like feature two miles wide would be mappable, but a tectonic event that moved the entire survey area up/down would not be detectible from the seismic data alone (but a wider, well-based interval mapping could reveal such a feature).

5.2 Tectonostratigraphic Intervals

Tectonostratigraphic intervals were established using significant reflections that were selected based on high continuity and robust amplitude. Figure 2 depicts these intervals relative to stratigraphy and the seismic data. The tectonostratigraphic intervals were initially designated in survey WC, and they are referred to as "TSI-1," "TSI-2," "TSI-3," and "TSI-4." The tectonostratigraphic interval breakdowns are as follows: TSI-1 is the oldest (and therefore the deepest interval) and its basal surface is at the Mississippian-Pennsylvanian Unconformity, or "MPU" while its upper surface is at the Oswego limestone horizon. TSI-2 is bounded by the basal Oswego limestone horizon and bounded above by the Osage Layton sandstone horizon. TSI-3 has the Osage Layton sandstone as a basal surface and upper surface of the Endicott-Oread horizon. TSI-4 is bounded below by the Endicott-Oread horizon and above by the Pawhuska limestone reflection event.

5.3 Isochron Maps and Horizon Flattening

The tectonostratigraphic sequences seen in survey WC also exhibit time-thickness variation. Isochron maps displaying the time-thickness of each TSI were constructed in order to quantify the time-thickness variations within the TSIs. Individual horizon-horizon isochron maps were also created to quantify the time-thicknesses between each horizon pair. It is important to note that while the contour interval on each isochron map is the same (5ms), the color bar scale is different for each map. This difference is attributed to the variation in the range of time-thickness between each interval that is being evaluated. For example, the color bar scale for the TSI-1 isochron map (Figure 10A) has a minimum value of 28 ms and a maximum value of 81 ms whereas the color bar scale for TSI-2 isochron map (Figure 13A) has a minimum value of 99 ms and a maximum value of 128 ms.

Basic interpretation of isochron maps like the one in Figure 12 follows from the assumption that the top horizon defining the interval represents a geologic marker at depositional slope. The general dip of the study area is, and has been, down to the SW into the Anadarko Basin except for paleokarst topography on the Mississippian-Pennsylvanian unconformity during the period of geological time studied. The tectonic alterations to this regional dip are the subject of this study. As the deepest interval studied, Figure 12A is influenced by the MPU topography which dominates the isochron variations observed. Even so, a general statement can be made that isopach thins represent paleotopographic high areas and isopach thicks are associated with paleotopographic low areas during the time interval of deposition of this tectonostratigraphic interval. Shallower intervals not influenced by the MPU will be interpreted in the same way—an isochron thin implies paleotopographic high and an isochron thick implies paleotopographic low—and considered in relation to the regional tectonic features discussed above.

Each isochron map has been paired with two seismic lines displaying the horizons of the tectonostratigraphic interval that is being focused upon. The interval represented in each map is highlighted on a seismic line taken from an angle that is orthogonal to the trend of the main feature(s). Some of these lines were taken using an arbitrary line function in Petrel, and some were taken from the original inlines and crosslines. In each case, the seismic line is shown unflattened (representing the tectonostratigraphic interval), flattened on the basal horizon, and also flattened on the top horizon. This is done to show the potential interpretation of two different possible settings. These flattened and unflattened seismic lines help highlight important tectonic and sedimentological features that are present within each interval.

5.4 Time-Thickness to Measured Depth-Thickness Conversion

Because isochron maps are made by measuring time-thickness of a specific interval in two-way travel time, a conversion must be made in order to estimate a measured depth-thickness similar to an isopach map. The first step in this conversion is to use the following equation:

$$z = v (t /2)$$

to estimate interval thickness (z, feet) given the interval velocity (v, feet/sec) and interval two-way travel time (t, seconds). In principle, the interval velocity will vary laterally and vertically across the survey area, but here we use 15,000 ft/sec (estimated from well A) for all Pennsylvanian interval thickness conversions.

The next step in the conversion process is to take the individual time-thickness values from discreet points on the isochron maps (t) and known velocity (v), to estimate thickness (z).

In practice, only maximum and minimum interval thicknesses will be calculated and reported. The conversion will allow for more accurate interpretations to be made with regards to the scale of the structures in question.

5.5 Finding the Trend of Regional Features

In order to find the trend of regional features in the isochron maps, a 360-degree protractor was overlain on top of the maps where a generalized line of trend was ascribed and measured using the azimuthal convention (0^{o}-360^{o}, North=0). All trend measurements given in this study are approximate trends relative to due north.

6. Observations

6.1 WC 3D Seismic Survey

6.1.1 Tectonostratigraphic Interval 1 (TSI-1) MPU to Oswego Limestone

Figure 10A is the time-thickness map of TSI-1 across the WC survey. This interval consists of one internal horizon, the Pink Lime. The maximum time-thickness value in this isochron is 81 ms (608 ft), and the minimum time-thickness value is 28 ms (210 ft). The thickest regions in this interval are in the southwest corner of the WC long with a similarly thick region in the north-central portion of the survey. There is apparent thinning in the northeastern and the northwestern corners of the survey, while the more central regions exhibit a relatively moderate thickness.

As can be seen on the seismic lines displayed for TSI-1 (Figure 10B,C), three horizons are grouped in the interval. The lowest of which is the Mississippian-Pennsylvanian Unconformity (MPU) (lower purple horizon), which is under the Pink Lime (green horizon) and overlain by the Oswego Limestone (upper purple horizon). The unflattened line (Figure 10B) shows a slight inclination dipping from north to south. When looking at the seismic data, thickness variation can be seen on both of the flattened versions of the line (Figure 10C,D). There is, however, a significant amount of reflection discontinuity that can be attributed to irregularity seen in the MPU, which is a paleokarst environment subject to carbonate dissolution in the subsurface.

6.1.2 MPU-Pink Lime within TS-1

The first horizon pair isochron map in TSI-1 is taken from the MPU up to the Pink Lime horizon (Figure 11A). The maximum time-thickness value in this isochron is 54 ms (405 ft), and the minimum time-thickness value is 2 ms (15 ft). In this time-thickness map, similar thickening patterns can be observed as those seen in the composite TSI-1 isochron map (Figure 11A). Significant thickening can be seen in the southwest corner of WC as well as in the north-central region. The thinnest portions of the map are again in the northeast and northwest corners, but in this specific horizon-horizon pair, the thinning is considerably more than in the TSI-1 composite. The southern portion of the map also depicts a thinner, more uniform interval than the TSI-1 composite.

The seismic line of Figure 11B is of the same orientation (N-S) as the seismic lines in Figure 10 and shows very similar features. There is a north to south inclination that appears to thicken in the same direction. This thickening is highlighted nicely in the flattened seismic lines (Figure 11C,D). Just as the TSI-1 composite interval showed discontinuous reflection in the flattened seismic line due to the presence of the MPU (lower purple horizon), the flattened line for the Pink Lime-MPU interval also shows these same electrocardiogram-like variations in reflection continuity.

6.1.3 Pink Lime-Oswego within TS-1

The Pink Lime to Oswego isochron interval shows a much more uniform time-thickness trend than the MPU to Pink Lime interval (Figure 12A). The maximum time-thickness value in this isochron is 36 ms (270 ft), and the minimum time-thickness value is 13 ms (98 ft). There is a slight discontinuous pattern associated with the thickest intervals. The most elongate of the thicks are located on the flanks of the thinnest interval in the northeast. When moving from east to west on the map, the thicks become more isolated and less elongate than in the east. The largest single thick entity is again in the southwest, but it is significantly smaller and more isolated than the previous horizon-pair isochron. Nevertheless, the thickness variations seen in this interval are very subtle, and this could be attributed to the overall thin interval.

This interval is the first that is not affected by the irregularities presented by the MPU during the flattening process. From west to east, there is little variation in thickness on this seismic line (Figure 12B). The slightly dipping character seen on the west to east profiles in the study area are also seen here. When this line is flattened on the Pink Lime (middle green horizon), a mounded, thickened feature can be seen (Figure 12C). When flattened on the Oswego (upper purple horizon), this same thickening region in the west can be seen, but it is instead represented by a wedge-like trough (Figure 12D). This bump can also be seen in the map of Figure 12A as the southwestern thicker zone in the map.

6.1.4 Tectonostratigraphic Interval 2 (TSI-2) Oswego Limestone to Osage/Layton

The time-thickness of TSI-2 displayed in Figure 13A is a composite isochron of the interval from the Oswego limestone up to the Osage/Layton sandstone. It consists of three internal horizons, the Big Lime (yellow), horizon 500 (green), and horizon 439 (cyan). The maximum time-thickness value in the tectonostratigraphic interval 2 (TSI-2) isochron is 128 ms

(960 ft), and the minimum time-thickness value is 99 ms (743 ft). This interval shows a general thickening trend from northwest to southeast, with the thickest region in the southeast. This trend can be broken into three distinct thickness zones beginning with the thickest zone in the southeast, then a moderately thick zone across the southwestern-most corner to the northeastern-most corner of the survey, and then finally the thinnest of the three zones in the northwestern corner. The thickening to the southeast has a uniform linear trend that extends on its long axis from northeast to southwest, perpendicular to the general thickening trend (Figure 13A). The thickest interval in the southeastern corner of the survey shows a relatively continuous, uniform thickness (on the order of ~900 ft to ~960 ft). The intermediate interval also displays a linear trend from southwest to northeast, however it is not quite as uniform with its thickness—the northeastern potion of this zone has a more uniform thickness with some relatively thinner zones in isolated areas, but to the southwest, the uniformity breaks down into a more splotchy pattern of semi-isolated patches of similar thickness. The semi-isolated patches of intermediate thickness in this zone still exhibit an elongate, linear trend from northeast to southwest. The third, thinnest unit in this composite isochron is in the northwestern-most corner of the survey, ranging from ~740 ft to ~760 ft in thickness. This thin portion of the map is isolated, and it borders the edges of the survey. It shows a dramatic thinning trend from the previous unit.

Figure 13B exhibits an unflattened seismic line from NW to SE. The overall structure is that of a slightly inclined interval of reflectors dipping from east to west at an approximate maximum angle of 1.6°. This inclination could potentially be attributed to the uppermost boundary of TSI-2, the Layton/Osage sandstone, which also serves as the basal horizon of TSI-3 or Clinoform Zone. The flattened seismic lines (Figure 13C,D) illustrate the thickening trend seen on the isochron map for the TSI-2 composite. The seismic line that is flattened on the basal

Oswego horizon (purple) shows the thickening in the SE as a subtle mounded feature (Figure 13C). The line flattened on the uppermost horizon of the interval, Osage/Layton (red), shows a wedge-like trough thickening pattern to the SE (Figure 13D). Both of these lines are representative of the southeasterly thickening trend shown on the isochron.

6.1.5 Oswego-Big Lime within TSI-2

The first horizon-pair isochron map for TSI-2 features the Oswego (lower purple) up to the Big Lime (yellow) interval. The maximum time-thickness value in this isochron is 26 ms (195 ft), and the minimum time-thickness value is 5 ms (38 ft). This isochron interval exhibits an almost entirely uniform time-thickness as can be seen in Figure 14A. This map is at, or near vertical resolution. As a result, there are a number of E-W “thickness artifacts”. There are, however, a few anomalous regions of the map showing distinct thickening and thinning trends. The most notable region of this map is the western-most portion; there are two large dome-shaped areas that exhibit a thickening trend in the south and a thinning trend directly adjacent to the north. The thicker unit shows a semi-continuous, semi-uniform unit that is abruptly truncated and bordered by the thinner, more continuous unit to the north. In the eastern portions of this isochron map there can be seen some isolated thick splotches that are seemingly randomly spaced within the most uniform regions of the survey.

Figure 14B is an unflattened seismic line that runs from north to south along the western margin of the map, highlighting the main features described above. There are multiple small undulations in the Big Lime horizon, which could potentially be caused by the nature of the 3D autotrack method for this particular horizon. The interval thickness seen on the seismic line is, however, relatively uniform aside from the thin to thick transition seen in the westernmost region of the map (Figure 14A). The seismic line flattened on the basal Oswego horizon (purple) shows a steady thinning gradient from north to south that is consistent with the isochron map (Figure 14A,C). Once the thinnest region of the line is reached, however, the transition into the thickest portion of the interval occurs. Here, a mounded geometry can be seen in Figure 14C. Figure 14D is the line flattened on the upper horizon 500 (yellow), and at the transition point from thinnest to thickest there is a wedge-like geometry that is seen.

6.1.6 Big Lime-Horizon 500 within TSI-2

The time-thickness map of the Big Lime (yellow) to horizon 500 (green) is shown on Figure 15A. The maximum time-thickness value in this isochron is 26 ms (195 ft), and the minimum time-thickness value is 3 ms (23 ft). It is immediately apparent that there is far less uniformity in this interval relative to some of the previous intervals. There are still some trends that can be observed, the first of which is the overall thinning to the south and southwest of WC. The southwest corner of WC is significantly thinner than in any other region of the map. There are some isolated thicks in the northern and western portions of the survey, but they are far less abundant than any of the other thinner intervals that are not part of the massive, globular thinning trend in the southern-most portion of the map.

This interval is also relatively thin, but it does show some thickness variation when looking at the seismic lines in Figure 15B,C,D. Horizon 500 (green) was also picked using 3D autotrack, so there are some picking discrepancies that can be seen in both flattened and unflattened seismic lines. These seismic lines run north to south in the western region of the mapped area. When moving from north to south, the interval transitions from relatively thin to quite thick, and then very thin in the southern region of the line. This thin region appears in an inverse of the trend seen in the previous horizon pair, where there was a relatively thin region was present in the middle of the line, and a thick region is immediately adjacent to the south (Figure 14).

6.1.7 Horizon 500-Horizon 439 within TSI-2

Figure 16A depicts the isochron map for the interval of horizon 500 up to horizon 439. The maximum time-thickness value in this isochron is 77 ms (578 ft), and the minimum time-thickness value is 19 ms (143 ft). This interval shows a trend just the opposite of the 500-Big Lime isochron map. The thinnest portions of the map are found in the northern half of the WC where the thickest regions are in the south half of the survey. The northern, thin half of the interval sees a generally continuous, uniform trend of thinning to the north where the thinnest areas are in the northwestern-most corner and the very far east of the map.

The 500-439 horizon pair also features two 3D autotracked horizons, so there are obvious discontinuities representing the aforementioned "electrocardiogram-like" responses in the horizons moving from north to south in the seismic lines (Figure 16B,C,D). Horizon 500 in particular has quite a few significant busts that are observable in the northern-central region of the unflattened seismic line, and these translate into busts on the flattened seismic lines. Aside from these minute sources of potential error in the horizon picking procedure, there is a relatively uniform thickness with little variation from north to south seen on the line. There are few changes in overall thickness that are not attributed to seismic character and horizon picking, as can be seen on the map in Figure 16A.

6.1.8 Horizon 439-Osage/Layton within TSI-2

This time-thickness interval shows a linear trend that is oriented northeast to southwest on its long axis (Figure 17A). This trend is similar to the TSI-2 isochron shown on Figure 13A.

The maximum time-thickness value in this isochron is 56 ms (420 ft), and the minimum time-thickness value is 4 ms (30 ft). The thickest zone is in the southeastern portion of the map. Moving northwest on the map (perpendicular to the overall linear trend), the thick zone transitions to a significantly thinner zone that expresses the same linear trend as the thickest zone. Continuing to the northwest, there is another transition into a smaller thick region. This thick region is not as widespread, and the thickest parts of the zone are to the northeast. There is a final transition to the northwest from thick to thin that is similar in nature to the middle thin zone. There is also an isolated thick zone in the farthest northwest corner of the map, which takes on the shape of a thickening band.

The final horizon pair of horizon 439 up to the Osage/Layton is shown on the seismic lines of Figure 17B,C,D. The busts in 439 that were discussed in the previous section also play a role in the character of the isochron map generated in Figure 17A, but they are not as significant due to the quality of picking on the Osage/Layton horizon. The lines shown in Figure 17 are of a northwest to southeast orientation, which is orthogonal to the trend of the lineated features seen in the isochron map. These lines illustrate the subtle oscillation of thick to thin that is seen in the isochron map. The unflattened line shows short wavelength structural undulations from northwest to southeast (Figure 17B). The variations in thickness are more readily observed when viewing the flattened lines (Figure 17C,D). Figure 17C is flattened on the basal horizon 500 (cyan), and Figure 17D is flattened on the Osage/Layton horizon (red).

6.1.9 Tectonostratigraphic Interval 3/Clinoform Zone (TSI-3 or CZ) Osage/Layton to Horizon 352

The composite isochron map for TSI-3 or "Clinoform Zone" is shown in Figure 18A. The base of this interval is the Layton/Osage sandstone (lower red), and the top is horizon 352 (orange). The maximum time-thickness value in this isochron is 96 ms (720 ft), and the minimum time-thickness value is 48 ms (360 ft). There is a strong NE-SW grain to this map that divides it into adjacent thick and thin regions. The thickest zone in this interval is in the southeastern-most portion of the study area and exhibits a semi-linear trend in the orientation of northeast to southwest. This trend is fairly apparent across the entirety of the map, and it defines the different zones that are present. Moving northwest, the study area shows a transition to thinner intervals, the thinnest of which is in the northern-most central region of the map. The thinnest zone shows a similarly elongate trend in the same orientation as the thickest zone to the southeast.

The Clinoform Zone is so named for its succession of clinoforms, the most pronounced of which in WC is the Avant Clinoform that was thoroughly investigated by Barker 2018. Figure 18B is the unflattened version of the seismic line with an orientation of northwest to southeast, highlighting the CZ, which consists of two horizons, the lowest of which is the Layton/Osage sandstone (lower red) and horizon 352 (orange).

6.1.10 Osage/Layton-Avant within TSI-3/CZ

The Layton/Osage up to the Avant is the first horizon pair interval of the Clinoform Zone is shown in Figure 19A. The maximum time-thickness value in this isochron is 79 ms (593 ft), and the minimum time-thickness value is 9 ms (68 ft). The first thing that can be seen is the extremely pronounced linear trend that is oriented from northeast to southwest on its long axis. Zones across the study area exhibit a trend of thinning from southeast to northwest, which is perpendicular to the linear trend that was just described. The thickest zone is in the southeastern region of the map. Three more distinct zones that are progressively thinner are apparent to the northwest. All exhibit the same elongate linear trend from northeast to southwest. To the northern end of the thickest zone, there is a hook-like feature that resembles a reentrant to the northeast. Continuing to the northwest the isochron map shows a trend of progressive thinning, with the thinnest zone of the study area in the northwestern corner of the map.

The Osage/Layton-Avant horizon pair represents the depositional packages below the structural top of the Avant Clinoform. In the unflattened seismic line (Figure 19B), the true Avant Clinoform structure can be seen, but in the flattened lines (Figure 19C,D), the time-thickness variations are very apparent—to the west-northwest (basinward), the interval is significantly thinner, moving up the slope (to the east-southeast), the interval gets progressively thicker, and finally once on the shelf (far eastern region), the thickest region of the seismic line is represented.

6.1.11 Avant-Horizon 352 within TSI-3/CZ

The second horizon pair interval in the Clinoform Zone is from the Avant horizon up to Horizon 352 (Figure 20A). The maximum time-thickness value in this isochron is 59 ms (443 ft), and the minimum time-thickness value is 8 ms (60 ft). This time-thickness map depicts a similar thickening pattern as the Osage/Layton-Avant interval, but it is inverted. From southeast to northwest there is a thickening trend, with a similar linear trend seen along the long axis of the zones with an orientation of northeast to southwest. For the Avant-352 interval specifically, it must be noted that the thinnest zone is in the entirety of the eastern portion of the map. Moving west-northwest, the study area thickens progressively. The thickest portion of the study area is in the northwest, and it is a relatively uniform thickening except for a bullseye that represents a relatively thinner area within the thickest region of the map.

352-Avant represents the interval of deposition post-clinoform development (Figure 20B,C). The most prominent feature in the CZ is the clinoform of Avant age (highlighted by the red horizon in the middle of the CZ interval in Figure 20B,C,D). The shelf slope break of this clinoform has a strike that extends north-northeast to the south-southwest (024°) in WC with the distal, basin-ward bottomset complex to the west and the proximal, top set complex to the east (Figure 20B). Above the distal bottomsets of the Avant clinoform reflectors representing younger sediment packages can be seen onlapping as they are truncated by the foresets of the clinoform (Figure 20B). The sediment packages associated with this clinoform exhibit thickening to the west and thinning to the east—patterns that are typically associated with the formation of a clinoform. The unflattened seismic line once again shows the true structure of the Avant Clinoform and its succeeding depositional units up to Horizon 352 (Figure 20B). Moving from west to east of Figure 20B, one can see the aforementioned onlapping sediment packages that are being truncated by the slope/foreset complex of the Avant Clinoform. Figure 20C highlights this interval from a flattened perspective, allowing for time-thickness variations to be observed and catalogued—moving from west to east, the interval exhibits a thinning trend. The westernmost (basinward) region of the line is the thickest part of the interval, and moving east, the interval progressively thins up the slope and onto the shelf, where the thinnest region of the interval is observed (Figure 20C).

6.1.12 Tectonostratigraphic Interval 4 (TSI-4) Horizon 352 to Pawhuska

The isochron for the final composite interval is TSI-4. This interval consists of five mapped horizons, in stratigraphic order, 352 (orange), 306 (lower red), 264 (lower green), 213 (upper red), and the Pawhuska limestone (upper green) (Figures 21-25). The maximum time-thickness value in this isochron is 179 ms (1343 ft), and the minimum time-thickness value is 142 ms (1065 ft). This composite interval exhibits an overall thickening gradient from southwest to northeast, which also exhibits a linear trend from northwest to southeast. In the southwestern-most region of the isochron, where the thinnest zones occur, there are two dome-shaped thin zones, the larger of which is in the far western portion of the map. The larger bulb to the west spans almost the entire western border of the map but begins to show a thickening trend to the north and the east of the bulb. The smaller of the two thin bulbs is in the south-central region of the survey. There is a small transition zone between the thin and thick zones. The thickest zones exhibit a similar dome-shaped, localized pattern. The larger of the two thicks is in the north-central region of the map and is mostly isolated. There is another localized thick zone in the southeastern corner of WC that is not as continuous as the northern thick zone, but still robust.

Figure 21B,C,D depicts the unflattened and flattened versions of the seismic line with the TSI-4 interval highlighted. This interval continues to exhibit a similar east-west thinning trend with reflectors dipping at an approximate angle of 1.5° at the shelf-slope break (Figure 21C). This is similar to that observed in the underlying CZ. There is a minor difference overlaying the onlapping depositional packages in the Clinoform Zone in the western region of the unflattened seismic line (Figure 21B). It is developed as a minor hump that is not present below the TSI-4 interval. This hump is diminished to nonexistent on the flattened profiles (Figure 21C,D). The flattened lines lend some insight into the composite time-thickness variations present in this final interval (Figure 21C,D), the first of which is a general thickening trend from west to east. There is a noticeable high that exists in what would be considered the shelf-slope break region of the line, indicative of a thick zone, which is also present on the map in Figure 21A. Moving eastward, the relative high is followed by a slight thinning point that then gives way to a progressive, gentle thickening trend to the edge of the survey (Figure 21C,D).

6.1.13 Horizon 352-Horizon 306 within TSI-4

Figure 22A exhibits the first individual horizon pair isochron of TSI-4 is from horizon 352 up to horizon 306. The maximum time-thickness value in this isochron is 63 ms (473 ft), and the minimum time-thickness value is 26 ms (195 ft). From south to north, this map displays a thickening trend with the thinnest portion of the map on the southern-most border of the survey. Moving north, there is a thickening gradient with the thickest zone in the far northwestern corner of the map. Overall, this map shows a relatively thinner interval, and the thinnest areas are the most widespread throughout the southern portion of the study area. There is also a generally continuous, less localized trend in this map as well—there are not many significant, isolated zones of thick or thin intervals.

The seismic lines featured in this interval run from north to south in at an angle that is orthogonal to the general east-west grain that is seen in the map of Figure 22A. The changes in interval thickness are apparent in even the unflattened seismic line—there is an obvious thinning trend to the south (Figure 22B). The flattened seismic lines (Figure 22C,D) for the 352-306 horizon pair interval also confirm the northerly thickening trend seen in the isochron map (Figure 22).

6.1.14 Horizon 306-Horizon 264 within TSI-4

The horizon pair isochron for horizon 306 up to horizon 264 is shown in Figure 23A. The maximum time-thickness value in this isochron is 60 ms (450 ft), and the minimum time-thickness value is 25 ms (188 ft). The thickening gradient seen here is different from that of the 352-306 isochron map in Figure 22A. In the 306-264 interval, a general thickening trend is exhibited from northwest to southeast, where the thinnest zones are in the northwest and the thickest zones are in the southeast. The gradient is relatively uniform with a few dome-shaped zones in the intermediate areas along the long axis of the trend, which runs from northeast to southwest. The largest thick zone is in the far southwest, and the largest thin zone spans the majority of the western and northwestern margins of the map.

When observing the seismic line flattened on horizon 306, a subtle but uniform thickening trend can generally be seen when moving from northwest to southeast across the lines (Figure 23C,D). The far northwestern region of the seismic lines represent the thinnest zone of the interval, and to the east there is a subtle thickening trend that seems to maintain a thickness in the realm of 39 ms (293 ft) to 42 ms (315 ft) of time-thickness until the very far southeastern region of the lines is reached, where the time-thickness increases significantly (Figure 23C,D).

6.1.15 Horizon 264-Horizon 213 within TSI-4

On the time-thickness map for the 264 to 213 interval, there is a significant amount of uniformity not seen in the other horizon pair maps for TSI-4 (Figure 24A). The maximum time-thickness value in this isochron is 62 ms (465 ft), and the minimum time-thickness value is 38 ms (285 ft). The majority of the map displays time-thickness values in the 42 ms (315 ft) to 50 ms (375 ft) range with some dome-shaped outliers in seemingly random regions of the map. The thickest of these outliers is a localized area in the southwestern region of the map. The thinnest of these outliers resides on the western and southern edges of the map, and there is also a localized thin zone on the northeastern edge of the map. A localized thick zone also exists in the northern-central region of the map.

264-213 shows a gradual thickening trend from northwest to southeast on the unflattened seismic section (Figure 24B). The southeasterly thickening trend seen in the seismic profiles is quite subtle, and does not show a large amount of variation except on the southeastern end of the seismic profiles where the interval is at its thickest (Figure 24C,D). The map in Figure 24A tends to follow this generalized trend seen in the seismic data—generally thin in the west, and generally thick in the east, a couple of isolated thicks and thins notwithstanding.

6.1.16 Horizon 213-Pawhuska within TSI-4

The 213 up to Pawhuska isochron map is the final horizon pair isochron map that is discussed (Figure 25A). The maximum time-thickness value in this isochron is 41 ms (308 ft), and the minimum time-thickness value is 14 ms (105 ft). Much like the 264-213 isochron map, 213-Pawhuska presents a uniform thickness distribution relative to the previous horizon pair isochron maps. The vast majority of the map exhibits a time-thickness distribution in the 20 ms (150 ft) to 28 ms (210 ft) range. There are some localized thick zones in the far eastern regions of the map that are situated on the edge of the study area. There are also some very localized thin zones concentrated in the far southeastern and northeastern corners of the study area, however they are extremely small and are moderately distanced from one another.

The seismic profiles of the final horizon pair interval of 213-Pawhuska exhibit a similar nonuniform time-thickness trend seen in the 352-306 flattened seismic line (Figure 22C and Figure 25C). There is much undulation moving from north to south in the unflattened seismic line (Figure 25B), and this high frequency variation is mirrored by the isochron map seen in Figure 25A. The location and orientation of this seismic line exhibits the subtle oscillation of thicks and thins in the eastern region of the map, but in the remainder of the mapping area to the west, there very little thickness variation (Figure 25).

7. Interpretations

The seismic lines and isochron maps that were discussed at length in the observations section of this investigation reveal clues regarding the presence of tectonic signals. This includes the identification of potential tectonic sources, the frequency of the tectonic pulses, the directionality of the pulses, and the effects of the pulses upon the sedimentation based on accommodation space seen on the Cherokee Platform during the Pennsylvanian interval. Some of these signals can be attributed to burial and compaction. These types of sedimentary signals will be of an even smaller scale than the already small-scale tectonic signals. When discussing accommodation space, the idea of a “see-saw” is invoked as a function of both sedimentological and tectonic influences on the study area and how they are related to the surrounding tectonic provinces. When interpreting the isochron maps, the thicker regions of the maps were considered to indicate potential structural lows, allowing for more accommodation space, and the thinner regions of the maps were considered to indicate potential structural highs with less accommodation space. It is important to note that the effects of erosion and internal unconformities are not immediately apparent when interpreting the isochron maps. These surfaces can be hidden below the resolution of the seismic data in some cases, and in other cases they can be seen and accounted for.

It is also important to keep in mind that the methodology for horizon picking varies from horizon to horizon—some horizons are continuous reflectors that allow for the use of an accurate 3D autotrack tool while others required a fully manual horizon picking method in order to accurately pick the correct reflector when partially buried in the noise of the seismic survey. The manually tracked horizons were picked on every ten crosslines and inlines to give an accurate horizon that could be interpolated during the gridding process and construction of time-structure and isochron maps.

7.1 WC 3D Seismic Survey

7.1.1 Tectonostratigraphic Interval 1 (TSI-1) MPU to Oswego Limestone

The composite TSI-1 interval, which is the base of the Pennsylvanian period, presents a special case in this investigation when interpreting time-structure and time-thickness maps along with the flattening of seismic lines because of the presence of the Mississippian-Pennsylvanian Unconformity. The MPU can complicate seismic interpretation because of its complex and highly variable nature as a paleokarst surface that has been subjected to multiple stages of weathering that can influence overlying seismic reflection events. In Figure 10, the paleokarst environment can be seen in the unflattened and flattened versions of the seismic line along with the isochron map that was constructed for the interval. The paleokarst structures still do not completely hide the structures that initially existed at the time of deposition of the younger units.

The map in Figure 10A shows thins in the northeastern and northwestern regions of the study area, indicating a contemporaneous structural high that featured little accommodation space in the context of the composite interval. The thickest region of the map in the southwest indicates a low that provided for a greater accommodation space. The high frequency irregularities in the thickness map are a product of the paleokarst environment, which results in local highs and lows in close proximity. A principle example of this is seen in the southwestern region of the map adjacent to the thickest (608 ft) region of the map, where a relative thin (~398 ft) exists directly to the north, and also to the immediate east, where another, thinner (~338 ft) region exists. One other occurrence of this phenomenon can be seen in the northernmost central region of the map, where the two thinnest (210 ft) regions of the map are punctuated by a relatively thicker (~465 ft) zone (when moving from west to east across the northernmost region of the map).

7.1.2 MPU-Pink Lime within TSI-1

The map of the Pink Lime down to the MPU seen in Figure 11A is strikingly similar to the map for the composite TSI-1 interval (Figure 10). This is a thinner interval that highlights structures caused by the paleokarst environment of the MPU. The discontinuous, pock-marked visualization of the thick and thin zones within the interval (upwards of 405 ft and 15 ft, respectively) is again interpreted to be a product of the paleokarst surface. Many of these features represent the discontinuous nature of the MPU's seismic character. As a result, there are many tracking errors in the MPU horizon. Because of these discontinuities in the seismic character there is little to be revealed from this map from a tectonic standpoint. Aside from the effect the MPU has on this interval, the thinnest regions of the map could most likely be attributed to compaction as they are on the scale of tens of feet, while the thickest zones could be a combination of edge effect and sea level fluctuation at the time of deposition.

7.1.3 Pink Lime-Oswego within TSI-1

This interval is the first horizon pair that is not in direct contact with the MPU (Figure 12). While the isochron map is still influenced by the MPU, there are also clues as to whether a structural or depositional control is in effect. There is a slight linear alignment with regards to the boundaries of the thin and thick regions in the eastern portion of the map. In the far eastern region, where the thinnest regions of the map exist, there is a northeast to southwest (037^{o}) trend of thin zones (~165 ft) followed by less continuous pockets of thick zones (~248 ft) along the same orientation. Further to the northwest the map begins to thin (~180 ft) again, depicting another relative high. The thins have been interpreted to be structural highs with less accommodation space, and the thicks are considered structural lows caused by peripheral tectonic activity. Although they are not as pronounced as on some of the later maps, the orientation of the strike of these lineaments is perpendicular to the azimuth of the compressive stresses of the Ouachita orogeny, which is southeast to northwest, relative to the study area. The crinkle effects become more prevalent as the Pennsylvanian interval proceeds, and the subsequent depositional troughs and lofts become more apparent. With that being said, it is far more reasonable to interpret this interval as the healing phase of the paleokarst environment represented by the MPU. This can be seen by the more uniform infill seen across the map, and also in the flattened seismic lines (Figure 12C,D). The erratic, discontinuous seismic character exhibited by the previous intervals is not present in the Pink Lime-Oswego interval. This evidence is consistent with a healing phase interpretation.

7.1.4 Tectonostratigraphic Interval 2 (TSI-2) Oswego Limestone to Osage/Layton

The composite TSI-2 isochron map in Figure 13 depicts a feature with a well developed thinning trend to the northwest that has an azimuthal trend on the long axis of the feature bearing northeast to southwest (052°). The southeast is characterized by a trough as the thickest zone on the map (~900 ft), and there is a relative high in the thinnest zone in the northwest (~758 ft). The long axis of these features is also perpendicular to the compressive stresses of the Ouachita orogeny, and has been interpreted as a longer wavelength feature that exhibits a more gradual thinning in the northwestern direction. The trough in the southeast is consistent with a down-warping product of the compressive stresses of the Ouachita orogeny, and it gives way to the thinned, structurally higher region of the study area in the northwest. So instead of seeing multiple cycles of thick to thin, there is just one steady low to high moving from southeast to northwest in this composite TSI-2 isochron. The flattened seismic lines in Figure 13C,D both show the thickening trend to the southeast, but the wedge-like geometry of the flattened line in Figure 13D points to a better representation of depositional history. Infill of the trough-like features seen on the profile flattened on the Osage/Layton (Figure 13D) are more likely because the mounded geometry shown in Figure 13C would be more consistent with a deepwater fan complex, which is not present in this system.

7.1.5 Oswego-Big Lime within TSI-2

Thickness trends in the Oswego to Big Lime isochron seen in Figure 14 are quite subtle relative to the composite TSI-2 interval, but there are two key regions of note. The first of which is in the far western region of the map where the thinnest area of the map (~40 ft) sits directly adjacent to the thickest region located to its south (~195 ft). The difference in these thicknesses is interpreted to be caused solely by burial and compaction of sediments. This determination was made on the basis of scale of sediment packages—where the tectonically controlled features are dominated by thicknesses and structural relief of 100s of feet, some of the features prominent in this map are on the scale of 10s of feet, which could be attributed to compaction. However, the data available for this project do not support compaction estimates and some of the features reported here could have compaction as well as tectonic origins.

7.1.6 Big Lime-Horizon 500 within TSI-2

This interval is similar to the Big Lime-Oswego interval in the regard that it is thin relative to most of the other intervals. The first thing to keep in mind for this interval is the discontinuous seismic character of Horizon 500 (Figure 15B,C,D). 3D autotracking this horizon has moderate to high uncertainty resulting in tracking errors that can mislead interpretation when viewing the isochron map (Figure 15A). The southern two-thirds of the isochron map show a broad thin interval with an isolated extreme thin of ~25 ft thickness in the far southwestern corner and a thicker interval ~195 ft to the north and east of the thinned zone. It is difficult to ascribe a definite tectonic origin to the features in this map due to the tracking errors and the interval thickness, so there will not be a suggestion as to whether or not there may be tectonic signals present.

7.1.7 Horizon 500-Horizon 439 within TSI-2

The 500-439 interval consists of two horizons that were picked using 3D autotracking methods, so it is important to note that there are some discontinuities within the seismic section, most notably in the 439 horizon (Figure 16). The thinning gradient that can be seen moving from south (where the thickest zones reach up to 580 ft in thickness) to north (where the thinnest of zones reach about 145 ft in thickness) does, however, present enough uniformity to ascribe a potential tectonic origin. The main gradient features a trend of 090°, which is also perpendicular to the Ouachita front compressional regime.

7.1.8 Horizon 439-Osage/Layton

This interval facilitates the return of certain tectonic overprinting in the Pennsylvanian interval as a prominent crinkle effect can be seen again (Figure 17). A general northeast to southwest trend along the azimuth 063° is visible throughout the isochron map with a relative thin (~158 ft) in the southeast moving northwest into what has been interpreted as a trough (thick) (~240 ft), back into a relative thin (high) (~175 ft), another less continuous trough (~235 ft), and finally back into another relative thin (~165 ft) in the far northwestern corner of the map. The thick zone in the extreme far northwestern corner of the map is interpreted as edge effect and has been excluded from this interpretation even though it fits the crinkle effect pattern. Flattening on the Osage/Layton horizon (red) in Figure 17D allows the interpreters to better view the trough structures that were filled in prior to the increased rate of sedimentation brought on by the development of the CZ. The 063° strike of the regional lineations that dissect the troughs and highs is perpendicular to the general directionality of the compressive stress regime of the

Ouachita orogeny, and it has thus been interpreted to be consistent with the potential of being a peripheral effect of said orogeny.

7.1.9 Tectonostratigraphic Interval 3/Clinoform Zone (TSI-3 or CZ) Osage/Layton to Horizon 352

TSI-3, or CZ, is an interval that is interpreted as exclusively having a tectonic overprint from Ouachita and Ouachita-related tectonism. Figure 18 depicts the composite isochron for the interval as well as the associated seismic sections. In the composite isochron map (Figure 18A), the semi-linear trend that was previously described has a trend of 067^{o} in the northeast to southwest direction—perpendicular to the compressive stress regime introduced by the Ouachita orogeny. The thickest zone seen in the southeasternmost region of the map (~685 ft) is not necessarily a product of downwarping or subsidence due to tectonic stresses so much as it has been interpreted as a proximal buildup of sediment in a larger, clinoform-dominated system. The CZ was subjected to large amounts of sedimentation from the Ouachita orogeny and also the development of the Ozark Dome, which is a by-product of the Ouachita orogeny itself. There is also ample evidence, although not shown in this composite isochron, that peripheral tectonism is coincident with the development of this interval.

The following internal horizon pairs helped determine which event (Ozark Dome or Ouachita orogeny) provided sediment supply and uplift/subsidence on the Cherokee Platform that facilitated the development of this Clinoform Zone. The CZ is the first of the composite Tectonostratigraphic Intervals that shows a "composite signal," where the composite TSI isochron shows tectonic control—in this case, from the Ouachita front—over the entire interval that is different than the tectonic control in the individual horizon pair isochron maps. This will be seen in the following interpretive sections as the Avant/Layton-Osage interval is affected by the Ouachita front, and the 352-Avant interval is affected by the Ozark Dome.

7.1.10 Osage/Layton-Avant within TSI-3/CZ

The first, and lowest, of the horizon pairings in the CZ is the Osage/Layton-Avant shown in Figure 19. The steady thinning trend moving from southeast to northwest features a strike that is 051° from northeast to southwest, and it is perpendicular to the compression of the Ouachita orogeny, which is ramping up to full throttle at this point in geologic time. The trough (~535 ft) in the southeastern region has been interpreted to be an analogue for a platform-based (distal) "foreland" basin caused by subsidence and downwarping from the incoming Gondwana/Llanoria plate. The antithesis of this subsidence is present to the northwest in the form of the relative thin (~90 ft) uplifted zone. Figure 19D shows a seismic line of the interval that is flattened on the Avant (upper red). Here, the down-warped or subsided trough to the southeast is readily visible. This structurally controlled depocenter allowed for the thicker zone to the southeast to infill and then be subsequently uplifted by the Ozark Dome (as will be discussed further in the next horizon pairing) to form the structural high necessary for the evolution of the prominent Avant clinoform.

7.1.11 Avant-Horizon 352 within TSI-3/CZ

The Avant clinoform described in the observations section is ripe with clues as to its origin and the presence of tectonism within the stable cratonic setting of the Cherokee Platform. First, it is immediately apparent that there must have been some kind of relative subsidence (in this case to the west), uplift (in this case to the east), or a combination of the two in order for a clinoform to manifest. The direction of the propagation of the Avant clinoform (generally east to west) details the direction from which the sediment supply was initiated, and therefore tells which regionally local tectonic event is the culprit behind the development of the clinoform.

As noted previously, the Ozark Dome is due east of the Cherokee Platform, and it forms one of the many (contemporaneous) tectonically active boundaries of the stable cratonic interior. It can be interpreted that the development of the Ozark Dome directly influenced the development of the Avant clinoform seen in the Wild Creek survey. The uplift of the Ozark Dome created an active sediment supply for the clinoform as well as structural relief on which the clinoform could build basinward to the west (Figure 20B,D), which is the site of the relative subsidence in this system. The total relief of the clinoform ranges from ~375 ft in other regions of the WC survey to ~570 ft in the seismic section in Figure 20B, allowing it to be classified as a shelf-prism clinoform, following the convention established by Patruno, et al., 2015. High frequency sea-level changes also influenced the production of the Avant clinoform. When looking basinward (to the west), there are multiple reflectors in the seismic data that show on-lapping sediment packages with a thickness of ~85 ft, indicating a lowstand to transgressive systems tract (Figure 20B,D). The more proximal erosional surfaces in the foresets and topsets that are typically associated with the lowstand to transgressive systems tract (and thereby associated with the onlapping sediment packages at the toe-of-slope region of the clinoform) are below the seismic resolution of the WC survey and are therefore assumed to be present at a higher resolution. Sediment bypass to the deep basin indicates that there was abundant accommodation space supplied by the subsidence to the west and the uplift to the east. Figure 20A is an isochron map that shows the time-thickness of the interval from the top of the Avant clinoform to the top of the Clinoform Zone (Horizon 352). It is apparent that the thickening seen in the northwestern region of the map is from the sediment dispersal caused by the Ozark Dome to the east—sediment supply created by relative uplift, sediment transportation basinward due to structural relief and relative subsidence to the west. When examining the flattened seismic line in Figure 20D, it is apparent that the composite interval time-thickness for CZ is consistent with a clinoform succession with a maximum relief of ~570 ft and sediment influx from the east-southeast to the west-northwest.

One last key interpretation from this interval is that of the reentrant in the western region of the thinnest zone. Looking along the southwestern edge of the reentrant, if a line is propagated in the northwest to southeast direction along this edge, it can be interpreted that there is some type of semi-listric shaped boundary with a general strike of 125°, that is consistent with the morphology of normal fault traces. This boundary is parallel to the orientation of the Southeastern Oklahoma Aulacogen, which was the cause of significant normal faulting in deep basement events. The boundary that has just been described has been interpreted as a reactivated fault that has a trace along the azimuthal bearing 125°.

7.1.12 Tectonostratigraphic Interval 4 (TSI-4) Horizon 352 to Pawhuska

The composite isochron map of the final tectonostratigraphic interval, TSI-4, is shown in Figure 21A. The thickening trend from southwest to northeast—the thinnest of the trend being in the southwest (~1095 ft) and the thickest of the trend being in the northeast (~1275 ft)—features a linear trend from northwest to southeast with an overall trend of 122°. This strike is perpendicular to the generalized direction of the compressive stress regime caused by the Wichita/Arbuckle uplift to the southwest of the Cherokee Platform, which was the last of the active orogenic events in the Pennsylvanian interval and was beginning to conclude its development at this juncture. It has been interpreted that the Wichita/Arbuckle complex had an overall impact but was somewhat limited in the intermediate sequences of TSI-4. This brings about another example of the invocation of the composite signaling idea. The TSI-4 composite isochron indicates tectonic control derived from the Wichita/Arbuckle complex, but the internal horizon pair intervals are affected by Ouachita and Nemaha tectonism. This composite overprinting is only possible if the tectonism ascribed to the composite feature is active during or after the time(s) of the tectonic events that affected the intermediate horizon pair intervals, which is the case in this particular example as the Wichita/Arbuckle Complex was active into the earliest Permian.

7.1.13 Horizon 352-Horizon 306 within TSI-4

The composite isochron for 352-306, shown in Figure 22A, is interesting because while there is a general thickening gradient from south to north, there is a direct gradient from southeast to northwest that features a longitudinal trend of 078°(NE-SW), which is perpendicular to the compression field of the Ouachita orogeny. This observation allows for the interpretation that this thin (~220 ft) to thick (~445 ft) transition from south to north is likely a product of the Ouachita Orogeny. The longitudinal trend of this thickening gradient is approximately west to east 088°perpendicular to the compressive regime of the Ouachita orogeny. These maps are indicative of a relic effect of the Ouachita orogeny because the map shows a ~031° azimuth compression trend, a ~089° azimuth compressional trend, and a 078°-trending thickening/thinning feature.

7.1.14 Horizon 306-Horizon 264 within TSI-4

The isochron map of the interval 264-306 in Figure 23A shows northwest to southeast trending gradient that transitions from thick (~400 ft) in the southeastern corner of the study area to thin (~235 ft) in the northwest. The trend of the lineated feature is 057°, which is also perpendicular to the compressive stresses of the Ouachita orogenic belt. This is most likely the origin of the subsidence to uplift transition seen in this interval. This trend is consistent with the other Ouachita-related signals seen in previous intervals, and it presents another long wavelength signal that reinforces connection the Ouachita Orogeny. The thin on the western edge of the isochron map can be seen along the entirety of the western edge (Figure 23A). This seemingly relative uplifting of the western edge of the map could potentially be attributed to the Nemaha Uplift. The trend seen along the western edge is consistent with the proximity of the Nemaha. Looking at the flattened seismic line in Figure 23D, one can see the gradual thinning sequence to the northwest. The wedge-like structure seen here is consistent with the previous intervals in the Pennsylvanian interval and is considered to be the more accurate representation of the two flattened horizon lines.

7.1.15 Horizon 264-Horizon 213 within TSI-4

Figure 24 focuses on the penultimate horizon pair in the Pennsylvanian interval of the study area, 264-213. In this late Pennsylvanian interval, tectonic activity seems diminished in the surrounding regions. A thin area (~310 ft) to the west may represent a paleotopographic high that could relate to the Nemaha Ridge which was active into the Permian. If this is the case, the trough-like features to the east, which show an overall thickening of ~435 ft, would be evidence of subsidence in conjunction with the uplifting of the western zones of the study area.

7.1.16 Horizon 213-Pawhuska within TSI-4

The final interval of the study area is the 213-Pawhuska horizon pair shown in Figure 25. This interval is relatively thin, ranging from 105-310 ft at its extremes and 150-210 ft over the bulk of the interval. While it does show some thickening trends in the southeastern region of the map (~188 ft), which may indicate depositional compaction rather than tectonic movement. This interpretation is based on the relatively consistent thickness seen across the study area for this interval.

8. Conclusions

The first, and most important result from this investigation is that 3D seismic surveys can be used in the interior of stable cratonic platforms to identify and characterize tectonic signals from peripheral tectonic events, and then use said tectonic signals to infer which tectonic event is associated with the signal. These interpretations allow for better understanding the influence of peripheral tectonic events on cratonic sedimentary processes and accommodation space in the interval(s) that are being investigated.

The current project reveals the Pennsylvanian interval in western Osage County has been chiefly affected by the Ouachita orogeny, which has been interpreted to have impacted nearly every interval in this investigation. The Ozark Dome is also a key contributor to the signaling seen in the Cherokee Platform province, and it has been interpreted to be the main contributor to the structural relief that allowed the Avant clinoform to develop in the aforementioned CZ. The Wichita/Arbuckle Complex is a key player late in the Pennsylvanian interval, specifically the TSI-4 composite interval leading to the idea of "composite signaling" as it affects the whole of the TSI-4 interval while not erasing the tectonic signals present in the intermittent horizon pair intervals. The Nemaha Uplift may have also had a tectonic influence in the later Pennsylvanian intervals. One of the more surprising elements uncovered was the interpretation of the reactivated normal faulting related to the Southeast Oklahoma Aulacogen seen in the CZ interval. The reactivated faulting is interpreted to have structural control on the accommodation space provided in the CZ interval—the zones situated on the downthrown hanging wall are thicker than the zones on the upthrown foot wall.

9. Future Work

This investigation suggests a new method of detecting subtle tectonic influence on cratonic stratigraphic intervals. Future work would be to more accurately and consistently map the 3D seismic surveys in the immediate vicinity of WC, namely the AN and GH surveys in order to see if interpreted tectonic signals persist away from the WC survey, and if so, are they in any way different? There has already been some low resolution isochron mapping in these surveys, but more careful analysis in light of this study is needed in AN and GH. For this study area, the results would benefit from estimating an interval velocity for each individual interval to more accurately convert time-thickness to actual thickness. This investigation was completed using a constant velocity for the entirety of the Pennsylvanian interval.

10. References

10.1 Journal Articles

Algeo, T. J., 1992, Continent-Scale Wrenching of Southwestern Laurussia During the Ouachita-Marathon Orogeny and Tectonic Escape of the Llano Block, *in* Lindsay, R. F., and Reed, C. L., (ed.), 1992 Field Seminar Guidebook, West Texas Geological Survey, p. 115-131.

Bass, N. W., 1942, PART 11. Summary of subsurface geology with special reference to oil and gas: p. 343-393.

Bass, N. W., W. R. Dillard, L. E. Kennedy, and H. B. Goodrich, 1942, SUBSURFACE GEOLOGY AND OIL AND GAS RESOURCES OF OSAGE COUNTY, OKLAHOMA: p. 21.

Bass, N. W., H. B. Goodrich, and W. R. Dillard, 1942, PART 10. Burbank and South Burbank oil fields Townships 26 and 27 North, Range 5 East, and Townships 25 to 27 North, Range 6 East: p. 26.

Brenner, R. L., 1995, Sequences and Cyclothems in Upper Portion of Cherokee (Middle Pennsylvanian, Desmoinesian), Mid-Continent, U.S.A.: p. 25

Campbell, J. A., and Northcutt, R. A., 2001, Petroleum Systems of Sedimentary Basins in Oklahoma, Oklahoma Geological Survey Circular, no. 106, p. 1-5.

Chenoweth, P., 1968, Early Paleozoic (Arbuckle) Overlap, Southern Mid-Continent, United States, AAPG Bulletin, v.52, no. 9, p. 1670-1688.

Clinton, R. P., 1957, The Geology of the Osage Country, Tulsa Geological Society Digest, v. 25, p. 126.

Cloetingh, Sierd, 1988, Intraplate Stresses: A New Element in Basin Analysis, New Perspectives in Basin Analysis, p. 205-230.

Cox, R. T., 2009, Ouachita, Appalachian, and Ancestral Rockies deformations recorded in mesoscale structures on the foreland Ozark plateaus: Tectonophysics, v. 474, no. 3–4, p. 674–683, doi:10.1016/j.tecto.2009.05.005.

Dewey, J. F., and J. M. Bird, 1970, Mountain belts and the new global tectonics: Journal of Geophysical Research, v. 75, no. 14, p. 2625–2647, doi:10.1029/JB075i014p02625.

Dolton, F. L., and Finn, T. M., 1989, Petroleum Geology of the Nemaha Uplift, Central Mid-Continent, AAPG Datapages, p. 1-32.

Dott, R. H., 1927, Pennsylvanian Paleogeography with Special Reference to South-Central Oklahoma, Oklahoma Geological Survey Bulletin, n. 40-J, p. 5-23.

Elebiju, O., Matson, S., Keller, R., Marfurt, K., 2011, Integrated geophysical studies of the basement structures, the Mississippi chert, and the Arbuckle Group of Osage County region, Oklahoma, AAPG Bulletin, v. 95, no. 3, p. 371-393.

Gay, S. P., 2003, The Nemaha Trend-A System of Compressional Thrust-Fold, Strike-Slip Structural Features in Kansas and Oklahoma, Part 1, Shale Shaker, July-August 2003, p. 9-17.

Gay, S. P., 2003, The Nemaha Trend-A System of Compressional Thrust-Fold, Strike-Slip Structural Features in Kansas and Oklahoma, Part 2, Shale Shaker, September-October 2003, p. 39-49.

Gould, C. N., and Wilson, R.A., 1927, The Upper Paleozoic Rocks of Oklahoma, Oklahoma Geological Survey Bulletin, No. 41, p. 5-66.

Granath, J. W., 1989, Structural Evolution of the Ardmore Basin, Oklahoma: Progressive Deformation in the Foreland of the Ouachita Collision, Tectonics, v. 8, no. 5, p.1015-1036.

Johnson, K. S., 2008, Geologic History of Oklahoma, Oklahoma Geological Survey Educational Publication, n. 9, p. 3-8.

Johnson, K.S., 1989, Geologic Evolution of the Anadarko Basin, *in* Johnson, K. S., (ed.), Anadarko Basin, 1988 Symposium: Oklahomoa Geological Survey Circular 90, p. 3-12.

Johnson, K. S., Northcutt, R. A., Hinshaw, G.C., Hines, K. E., 2001, Geology and Petroleum Reservoirs in Pennsylvanian and Permian Rocks of Oklahoma, *in* Johnson, K. S., (ed.), Pennsylvanian and Permian Geology and Petroleum in the southern Midcontinent, 1998 symposium: Oklahoma Geological Survey Circular 104, p. 1-19.

Johnson, K. S., Amsden, T. W., Denison, R. E., Dutton, S. P., Goldstein, A. G., Rascoe, Bailey Jr., Sutherland, P. K., Thompson, D. M., 1988, Geology of the Southern Midcontinent, Oklahoma Geological Survey Special Publication, n. 82, vol. 2, 60 p.

Keller, G. R., Cebull, S. E., 1973, Plate Tectonics and the Ouachita System in Texas, Oklahoma, and Arkansas, Geological Society of America Bulletin, v. 83, p. 1659-1666.

Klein, George, 1990, Pennsylvanian Time Scales and Cycle Periods, Geology, v. 18, p. 455-457.

Lomask, J., and A. Guitton, 2007, Volumetric flattening: an interpretation tool: The Leading Edge, v. 26, no. 7, p. 888–897, doi:10.1190/1.2756869.

McBee, William Jr., 2003, Nemaha Strike-Slip Fault Zone, AAPG Mid-Continent Section Meeting: 14 p.

McGilvery, T. A., Manger, W. L., Zachary, D. L., 2016, The Carboniferous of Southwest Missouri and Northwest Arkansas, Third Biennial Field Conference, AAPG Mid-Continent Section, v. 3, 239 p.

McKEE, E. D., and Crosby, E. J., 1975, Paleotectonic Investigations of the Pennsylvanian System in the United States, United States Geological Survey Professional Paper, no. 853, 200 p.

Mickus, K. L., and Keller, G. R., 1992, Lithospheric Structures of the South-Central United States, Geology, v. 20, p. 335-338.

Patruno, S., Hampson, G., Jackson, C., 2015, Quantitative characterization of deltaic and subaqueous clinoforms, Earth-Science Reviews, v. 79, no. 119, p. 80-113.

Perry, W. J., 1989, Tectonic Evolution of the Anadarko Basin Region, Oklahoma, U.S. Geological Survey Bulletin, v. 1866-A, p. A1-A19.

Raymond C. Moore (2), 1948, Classification of Pennsylvanian Rocks in Iowa, Kansas, Missouri, Nebraska, and Northern Oklahoma: AAPG Bulletin, v. 32, doi:10.1306/3D933C3B-16B1-11D7-8645000102C1865D.

Rogers, S. M., n.d., NEMAHA FAULT ZONE OKLAHOMA: p. 53.

Roy, A., Dowell, B., Marfurt, K., 2012, Characterizing a Mississippian Tripolitic Chert reservoir using unsupervised 3D seismic facies analysis and well logs: an example from Osage County, Oklahoma, SEG Las Vegas 2012 Annual Meeting, 5 p.

Shaulis, B. J., T. J. Lapen, J. F. Casey, and D. R. Reid, 2012, Timing and Rates of Flysch Sedimentation In the Stanley Group, Ouachita Mountains, Oklahoma and Arkansas, U.S.A.: Constraints from U-Pb Zircon Ages of Subaqueous Ash-Flow Tuffs: Journal of Sedimentary Research, v. 82, no. 11, p. 833–840, doi:10.2110/jsr.2012.68.

Suriamin, F., and Pranter, M., 2018, Stratigraphic and lithofacies control on pore characteristics of Mississippian limestone and chert reservoirs of north-central Oklahoma, Interpretation, v. 6, no. 4, p. T1001-T1022.

Snyder, F. G., 1968, Tectonic History of Midcontinental United States, UMR Journal, v. 1, no. 5, p. 65-77.

Subsurface geology and oil and gas resources of Osage county, Oklahoma, 1938a: doi:10.3133/b900.

Subsurface geology and oil and gas resources of Osage county, Oklahoma, 1938b: doi:10.3133/b900.

Subsurface geology and oil and gas resources of Osage county, Oklahoma, 1938c: doi:10.3133/b900.

Suneson, N. H., 2000, The Geology of the Tallgrass Prairie Reserve, Osage County, Oklahoma, an Introduction and Field Guide, Oklahoma Geological Survey, Open-File Report, p. 36.

Tedesco, S. A., n.d., COALBED METHANE AND SHALE GAS IN THE CHEROKEE BASIN: EMERGING FROM EXPLORATION TO EXPLOITATION: p. 26.

Thomas, William, 1983, Continental Margins, Orogenic Belts, and Intracratonic Structures, Geology, v. 11, p. 270-272.

Thorman, C. H., and M. H. Hibpshman, 1979a, Status of Mineral Resource Information for the Osage Indian Reservation, Oklahoma, Administrative Report, BIA-47 p. 60.

Thorman, C. H., and M. H. Hibpshman, 1979b, Status of Mineral Resource Information for the Osage Indian Reservation, Oklahoma: p. 60.

Walper, J. L., 1977, Paleozoic Tectonics of the Southern Margin of North America, Gulf Coast Association of Geological Societies Transactions-American Association of Petroleum Geologists, v. 27, p. 230-241.

Yates, T., n.d., Oklahoma Geologic History Part I: 87 p.

10.2 Book Articles

Houseknecht, D. W., 1986, Evolution from Passive Margin to Foreland Basin: The Atoka Formation of the Arkoma Basin, South-Central U.S.A., *in* P. A. Allen, and P. Homewood, eds., Foreland Basins: Oxford, UK, Blackwell Publishing Ltd., p. 327–345, doi:10.1002/9781444303810.ch18.

10.3 Theses

Bahram, I., 2015., Stratigraphic and Structural Analysis of Middle Atoka Formation in Aetna Gas Field, Franklin, Johnson and Logan Counties, Arkansas, Master’s thesis, University of Arkansas, Fayetteville, Arkansas, 82 p.

Benson, R. C., 2014, 3D Seismic Mapping of Probable Tripolitic Chert Bodies in Osage County, Oklahoma, Master’s thesis, University of Arkansas, Fayetteville, Arkansas, 88 p.

Denham, W. S., 2018, Subsurface Stratigraphic Interpretation of the Lower Atoka Formation, Northern Arkoma Basin, Arkansas, Master’s Thesis, University of Arkansas, Fayetteville, Arkansas, 86 p.

Jennings, Caleb, 2014, Mechanical Stratigraphy of the Mississippian in Osage County, Oklahoma, Master’s thesis, University of Arkansas, Fayetteville, Arkansas, 81 p.

Keeling, R. M., 2016, Stratigraphic Interpretation and Reservoir Implications of the Arbuckle Group (Cambrian-Ordovician) using 3D Seismic, Osage County, Oklahoma, Master's thesis, University of Arkansas, Fayetteville, Arkansas, 70 p.

Liner, K. M., 2015. An investigation of 3D Seismic Deep Basement Events in Osage County, Oklahoma, Master's thesis, University of Arkansas, Fayetteville, Arkansas, 94 p.

Radcliffe, D. H., 1918, The occurrence of oil and gas in Osage County, Oklahoma, Professional Degree thesis, 39 p.

Sparks, T. A., 2018, Controls on Fracture Distributions within Regional, km-Scale Folds, Master's thesis, Texas Tech University, Lubbock, Texas, 87 p.

Studebaker, E. W., 2014, Structural and Stratigraphic Transition from the Arkoma Shelf into the Arkoma Basin during Basin Subsidence; Arkoma Basin, Northwest Arkansas, Master's thesis, University of Arkansas, Fayetteville, Arkansas, 64 p.

West, Alexander, 2015, Pennsylvanian Subsurface Sequence Stratigraphy Based on 3D Seismic and Wireline Data in Western Osage County, Oklahoma, Master's Thesis, University of Arkansas, Fayetteville, Arkansas, 114 p.

Wittman, B., 2011, Subsurface Stratigraphy and Characterization of Mississippian (Osagean to Meramecian) Carbonate Reservoirs of the Northern Anadarko Shelf, North-Central Oklahoma, Master's Thesis, Baylor University, Waco, Texas, 76p.

10.4 Technology

dGB Earth Sciences, https://www.dgbes.com, accessed 8 October, 2020

11. Tables and Figures

Table 1: Survey parameters for the WC, GH, and AN 3D seismic surveys

	WC Survey	GH Survey	AN Survey
Area	45 sq. mi.	48 sq. mi.	46 sq. mi.
Bin Size	66 ft	110 ft	110 ft
Inlines	3632-4031 (399)	160-528 (368)	5272-5671 (399)
Crosslines	10876-11596 (720)	1-200 (200)	1-713 (713)
Dominant Frequency	58 Hz	65 Hz	55 Hz
Time Sample Rate	2 ms	2 ms	2 ms
Record Time	2.0 s	2.0 s	2.0 s

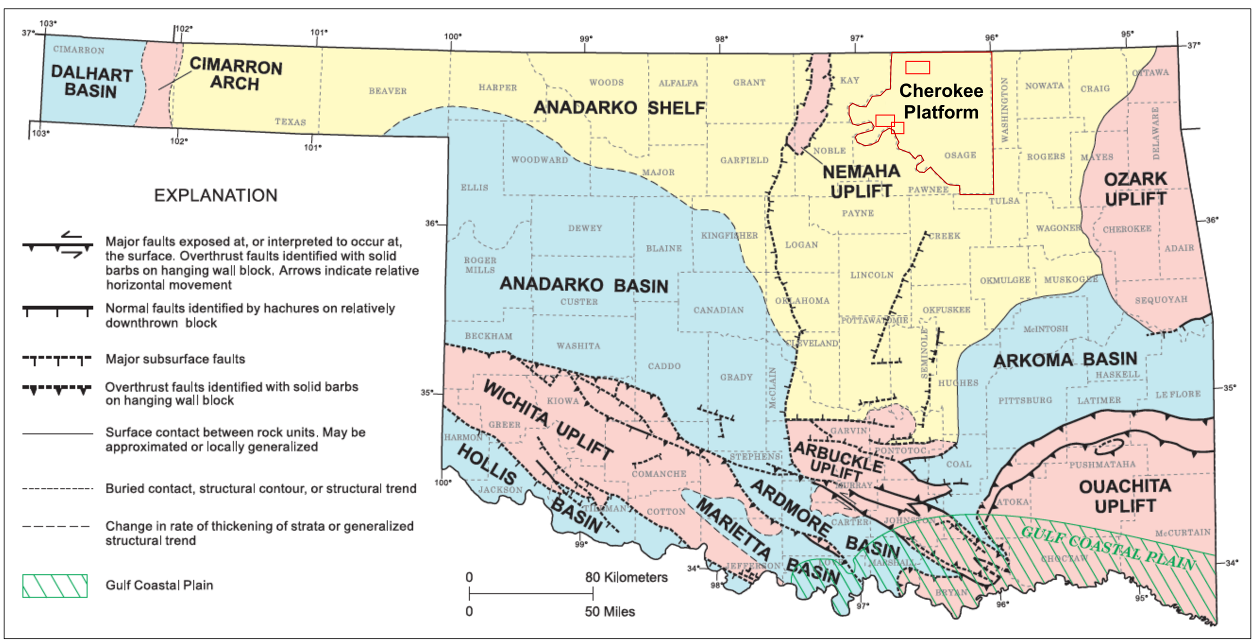

Figure 1: Map containing the geological provinces of Oklahoma including structural boundaries; red outline indicates the boundaries of Osage County and the 3D seismic surveys that are used in the investigation (Modified from Johnson, 2008).

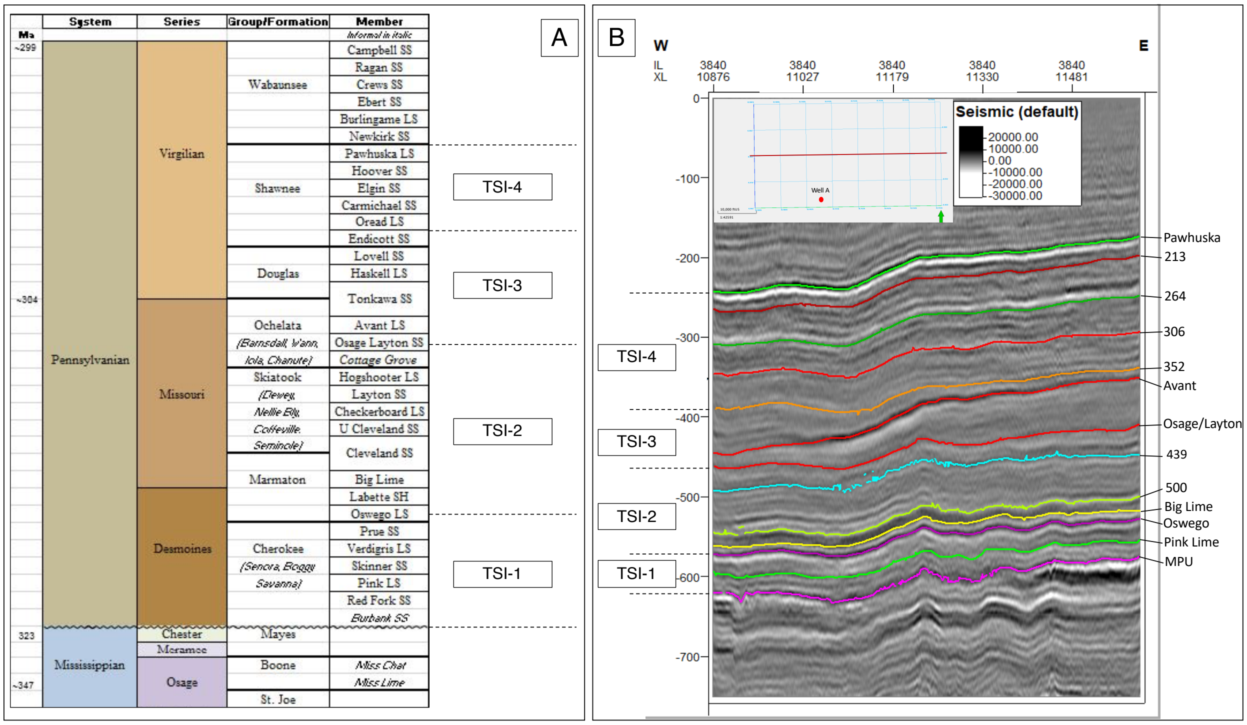

Figure 2: A) Stratigraphic column of late Mississippian and Pennsylvanian strata of western Osage County, OK. This stratigraphic column has been divided into tectonostratigraphic intervals by the investigators based on the seismic character of reflectors seen in B**; B)** Inline 3840 from WC with mapped horizons. This seismic line has been divided into tectonostratigraphic intervals that are based on seismic character and styles of interpreted tectonic activity.

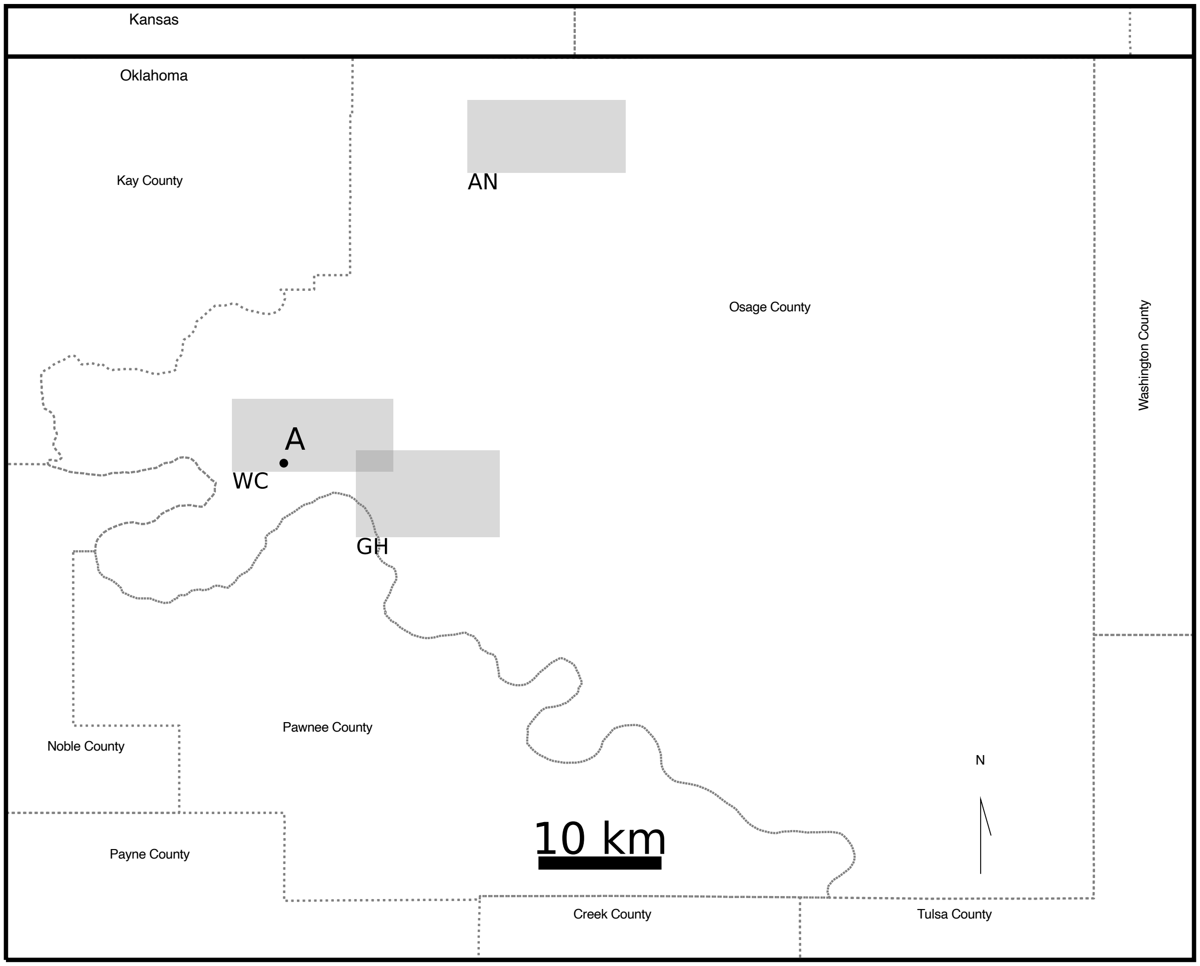

Figure 3: Enlarged map of the area within Osage County, Oklahoma. The 3D seismic surveys that are used in this investigation are indicated by the shaded boxes on the map; 3D seismic surveys are labelled WC, GH and AN. Well A is shown within the confines of WC (Python script courtesy of Lanre Aboaba).

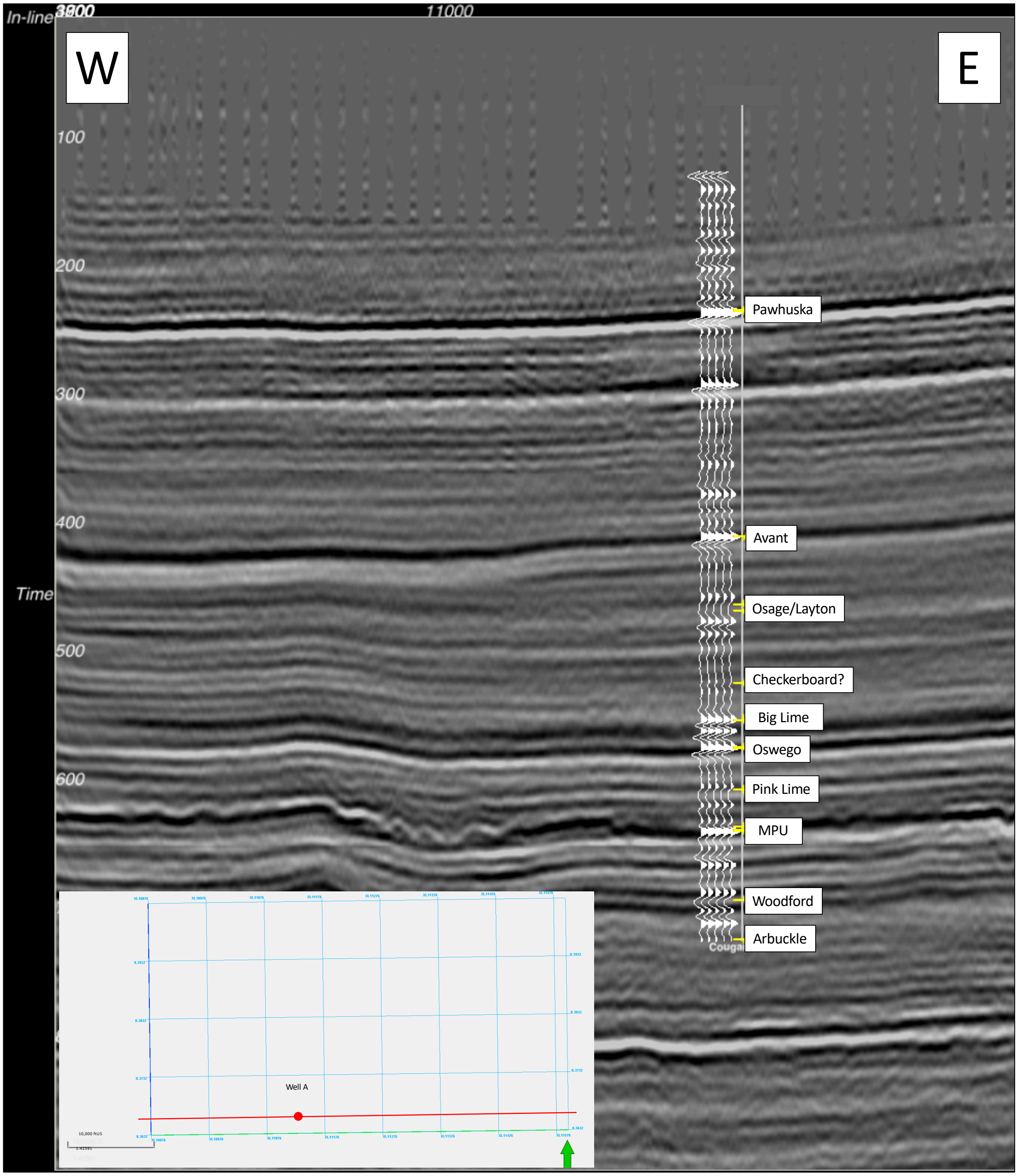

Figure 4: Synthetic seismogram tuned to the Pennsylvanian interval of WC (IL 3675). This synthetic is derived from sonic and density logs collected from the borehole of Well A.

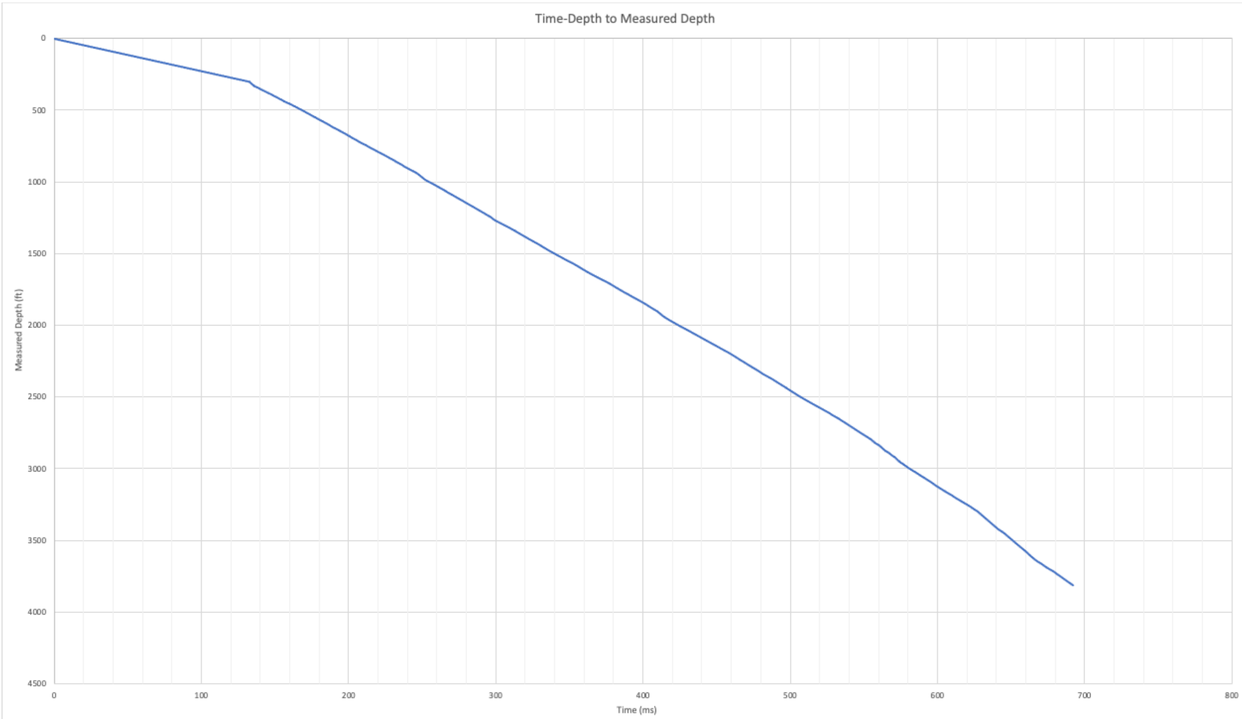

Figure 5: Time-Depth conversion curve for Well A used throughout 3D survey WC.

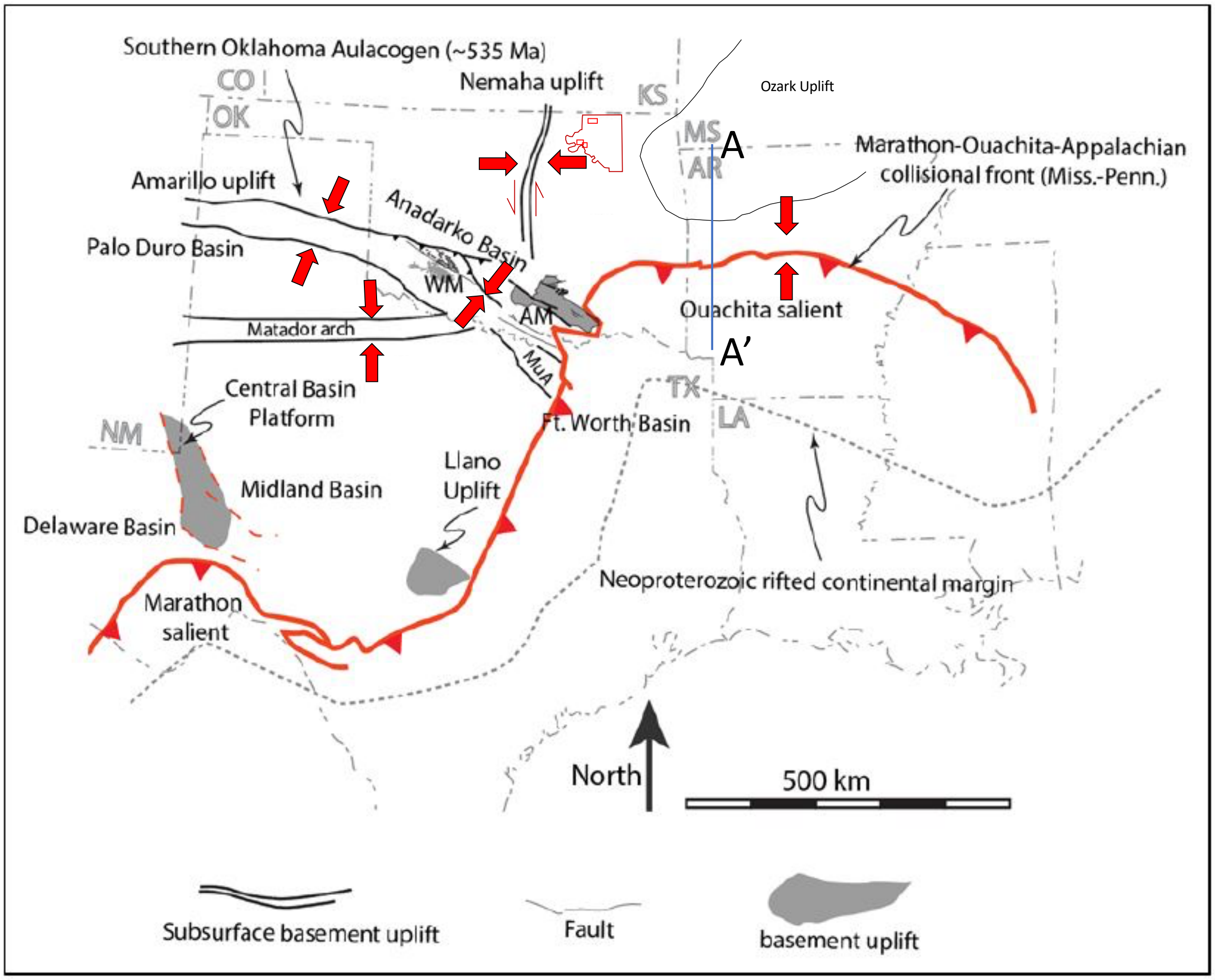

Figure 6: Map of the regional tectonics of the Ouachita Orogenic System including the peripheral tectonic elements of northwest Arkansas and Oklahoma. Arrows indicating the orientation of tectonic stresses applied to the study area are shown with red block arrows for compressional events, and thin red arrows indicating shearing events. A line of section for the tectonostratigraphic model in Figure 7 runs north to south in western Arkansas (modified from Sparks, 2018 via Ewing, 2005; Thomas, 2006).

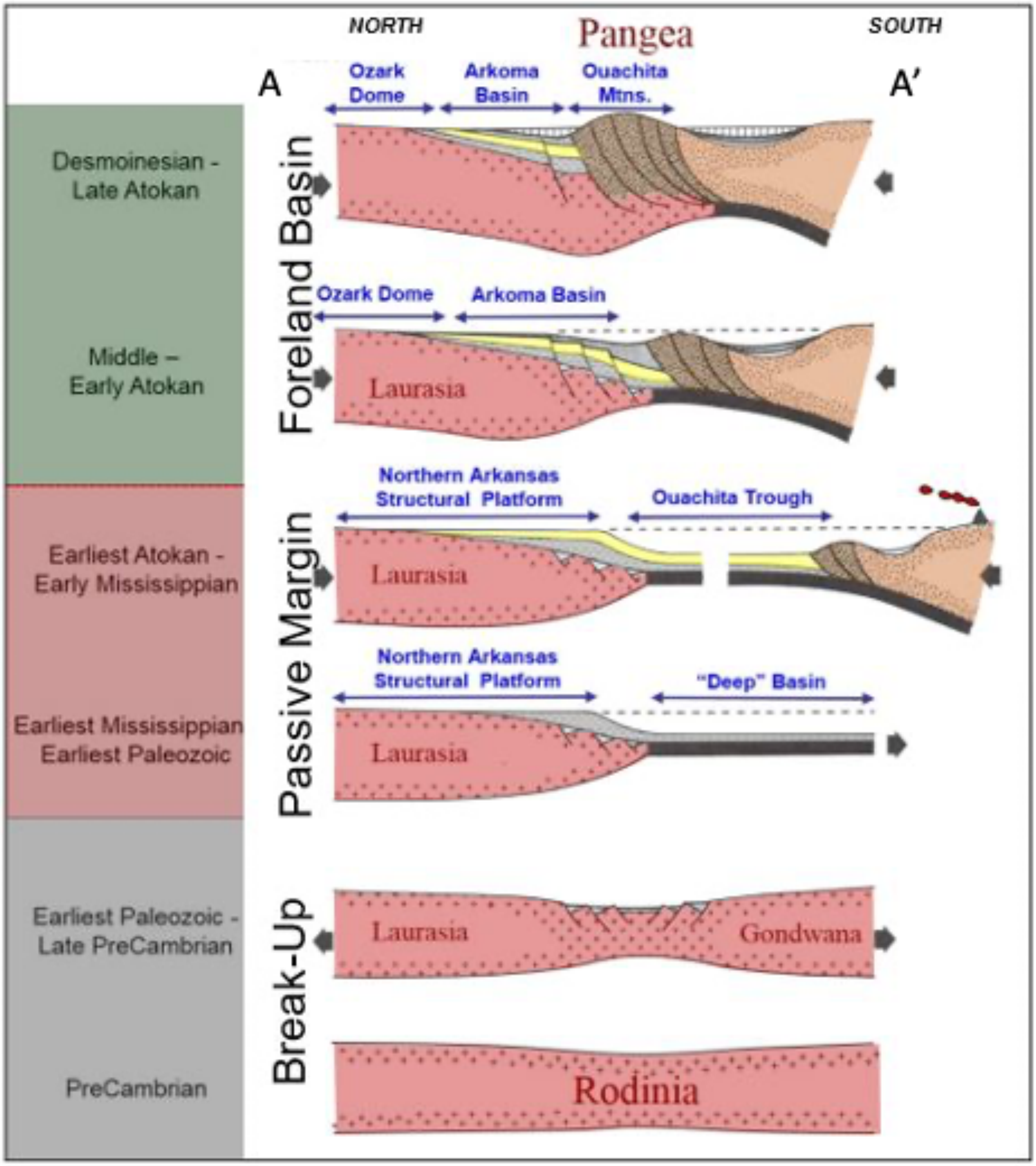

Figure 7: Working model of the tectonic evolution of the Ouachita mountains as it has been described by McGilvery, 2016 and Houseknecht, 1986. A to A' refers to the line of section in Figure 6.

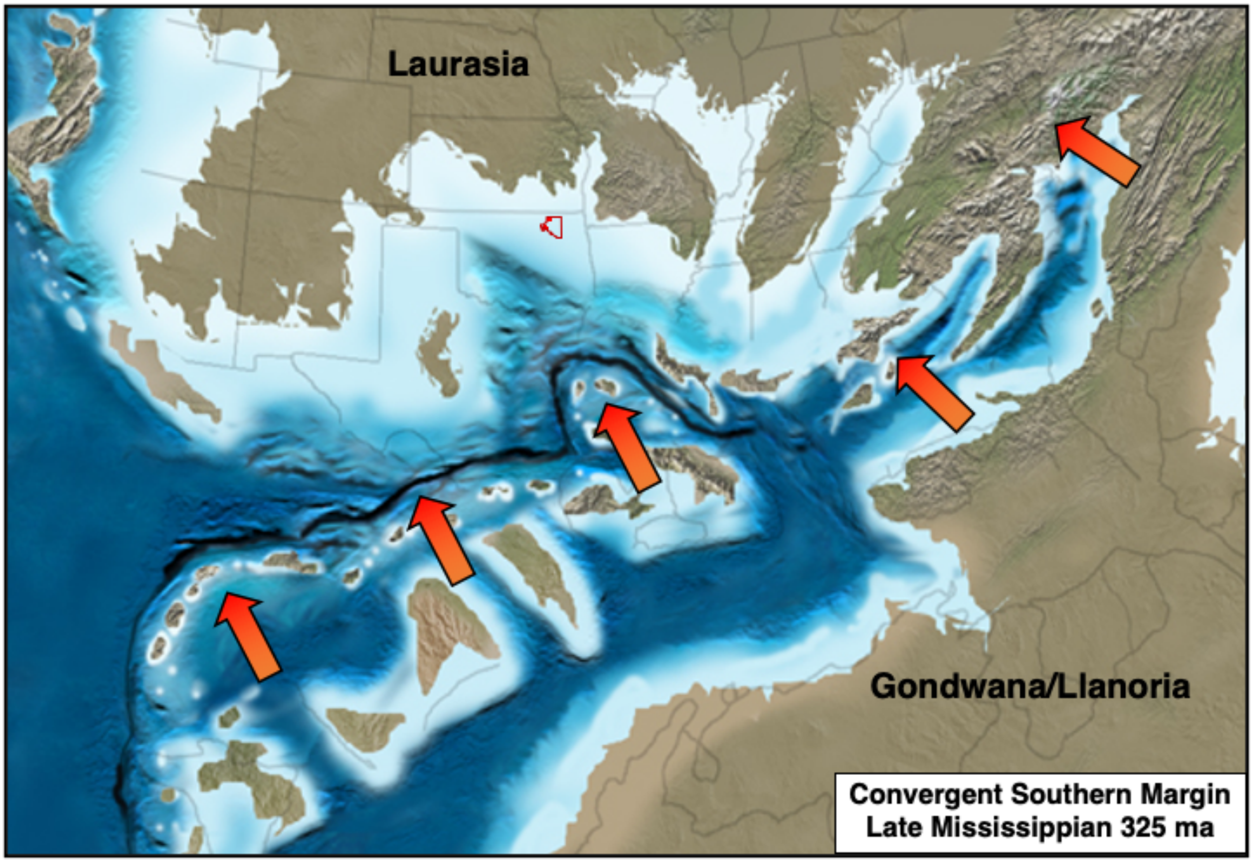

Figure 8: Blakey Map illustrating the convergent southern margin of Gondwana and Laurasia during late the Mississippian, ~325 ma. The red outline indicates the boundaries of Osage County, Oklahoma and the 3D seismic surveys that define the study area of this investigation (modified from Blakey, 2007)

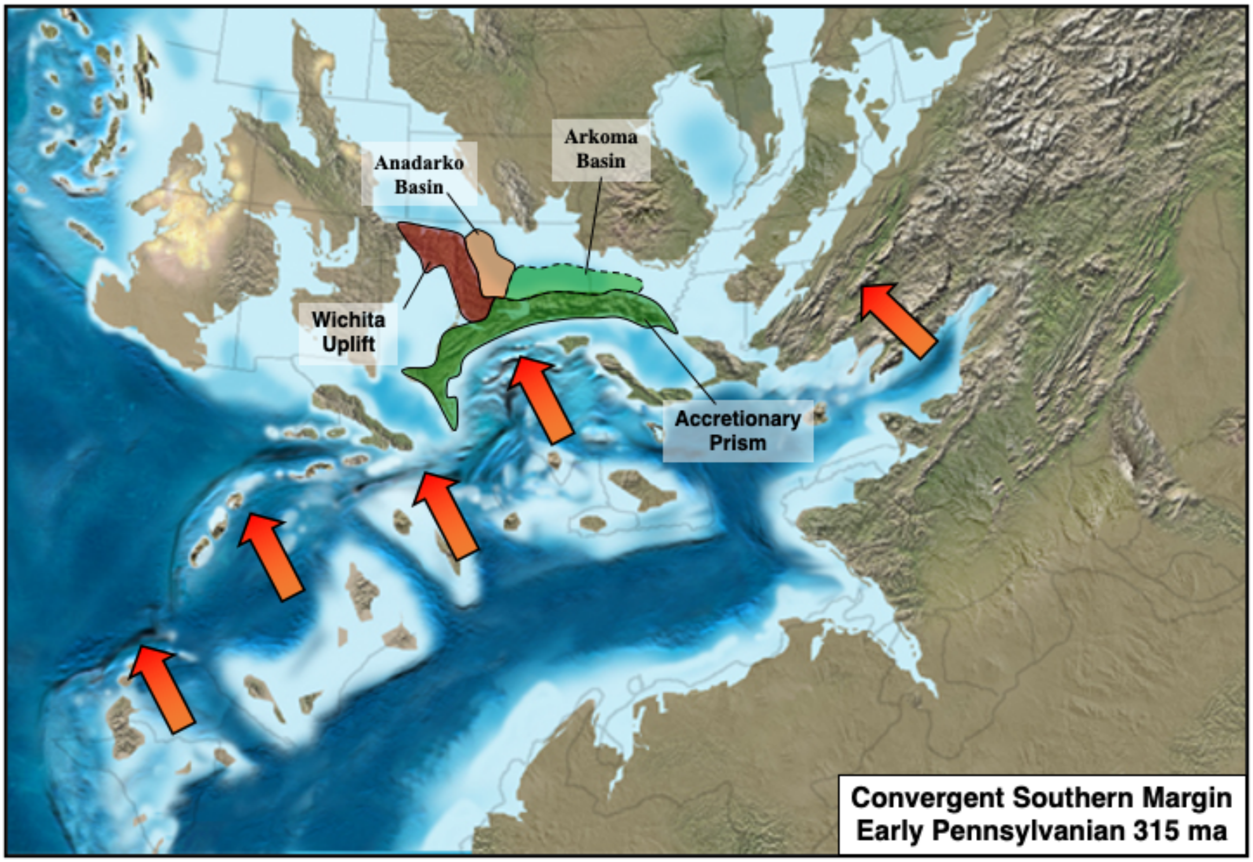

Figure 9: Blakey Map illustrating the convergent southern margin of Gondwana and Laurasia during the early Pennsylvanian, ~315 ma. The Ouachita accretionary prism, the Wichita uplift, and the proto-Anadarko and proto-Arkoma basins are superimposed on the map. The red outline indicates the boundaries of Osage County, Oklahoma and the 3D seismic surveys that define the study area of this investigation (modified from Blakey, 2007)

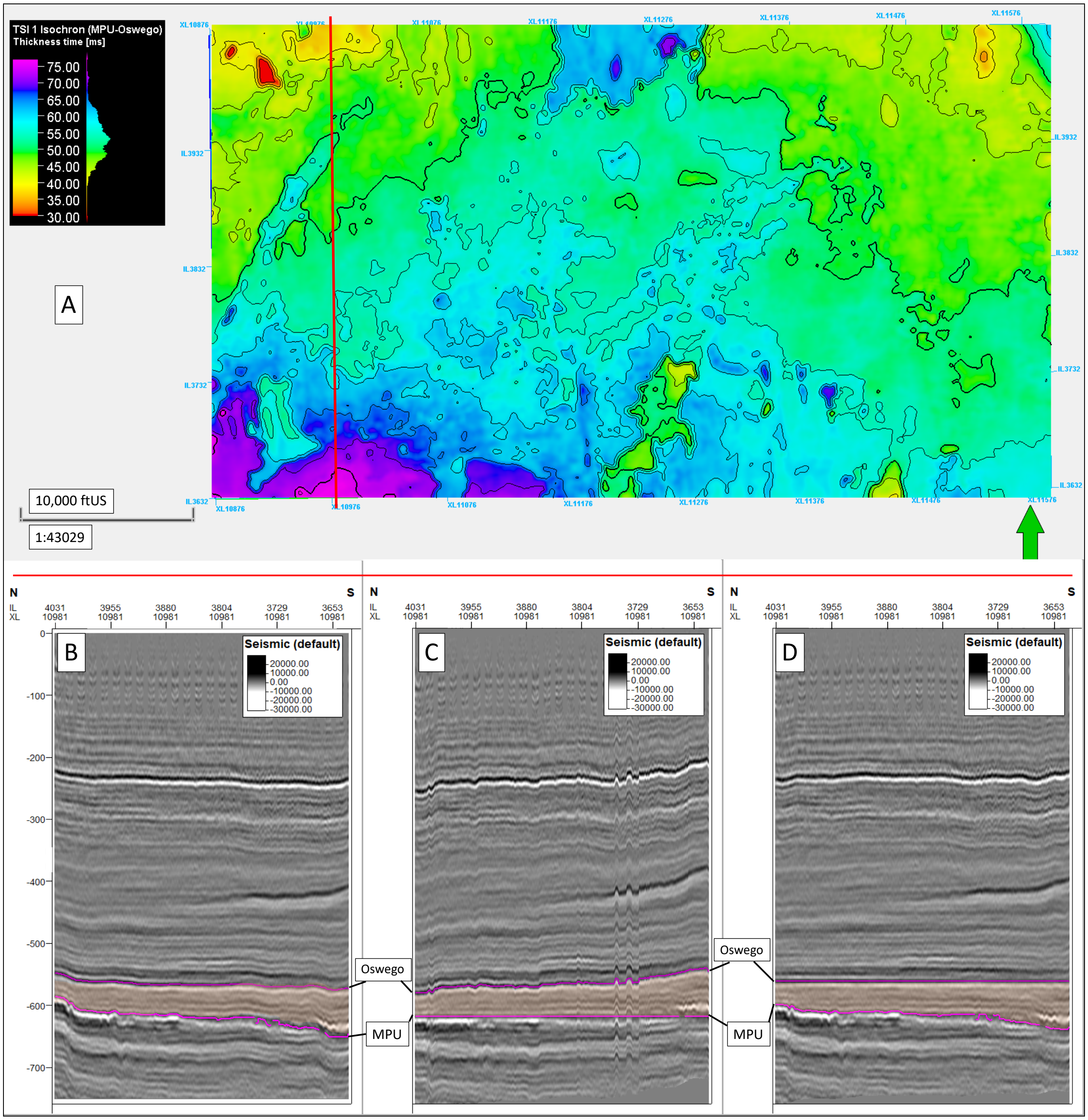

Figure 10: **A)** TSI-1 isochron map; **B)** Seismic profile from WC showing the unflattened horizons of TSI-1 with the isochron interval exhibited on the map in "A" highlighted; **C)** Seismic profile from WC showing the flattened basal horizon of TSI-1 with the isochron interval (MPU-Oswego) exhibited on the map in "A" highlighted; **D)** Seismic profile from WC showing the flattened upper horizon of TSI-1 with the isochron interval (MPU-Oswego) exhibited on the map in "A" highlighted.

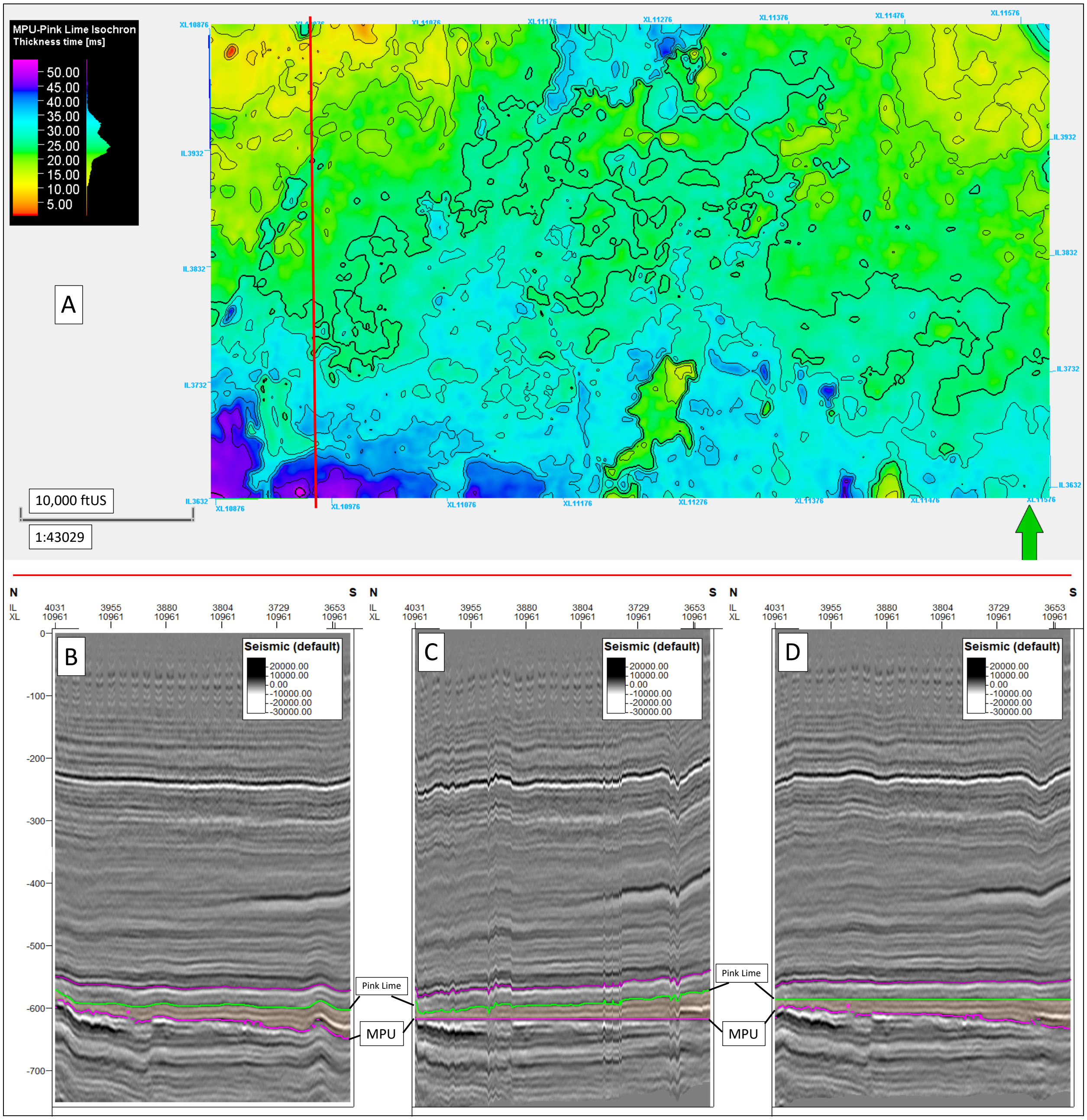

Figure 11: **A)** MPU-Pink Lime isochron map; **B)** Seismic profile from WC showing the unflattened horizons of TSI-1 with the isochron interval exhibited on the map in "A" highlighted; **C)** Seismic profile from WC showing the flattened basal horizon (MPU) with the isochron interval (MPU-Pink Lime) exhibited on the map in "A" highlighted; **D)** Seismic profile from WC showing the flattened upper horizon (Pink Lime) with the isochron interval (MPU-Pink Lime) exhibited on the map in "A" highlighted.

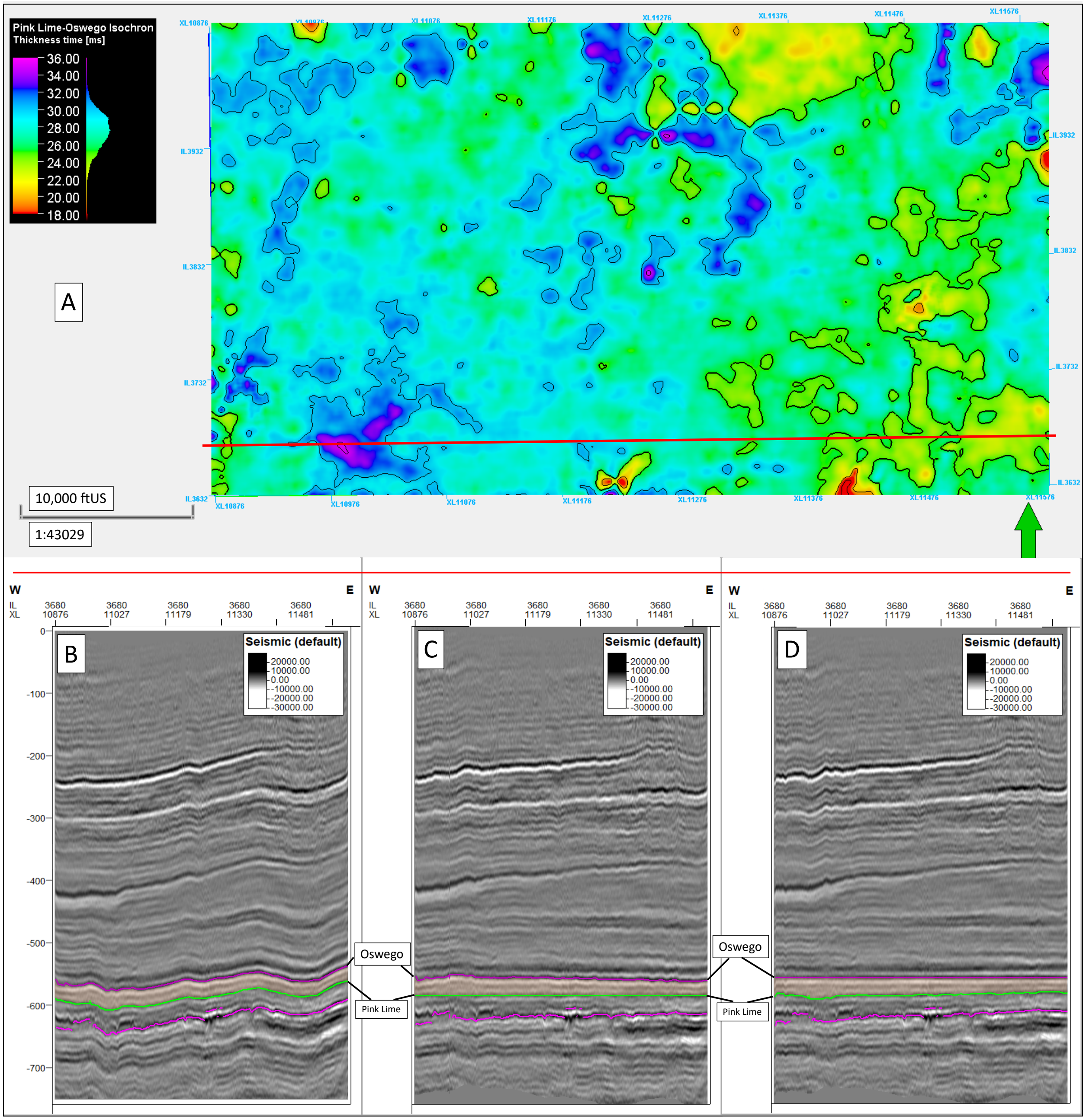

Figure 12: **A)** Pink Lime-Oswego isochron map; **B)** Seismic profile from WC showing the unflattened horizons of TSI-1 with the isochron interval exhibited on the map in "A" highlighted; **C)** Seisomic profile from WC showing the flattened basal horizon (Pink Lime) with the isochron interval (Pink Lime-Oswego) exhibited on the map in "A" highlighted; **D)** Seismic profile from WC showing the flattened upper horizon (Oswego) with the isochron interval (Pink Lime-Oswego) exhibited on the map in "A" highlighted.

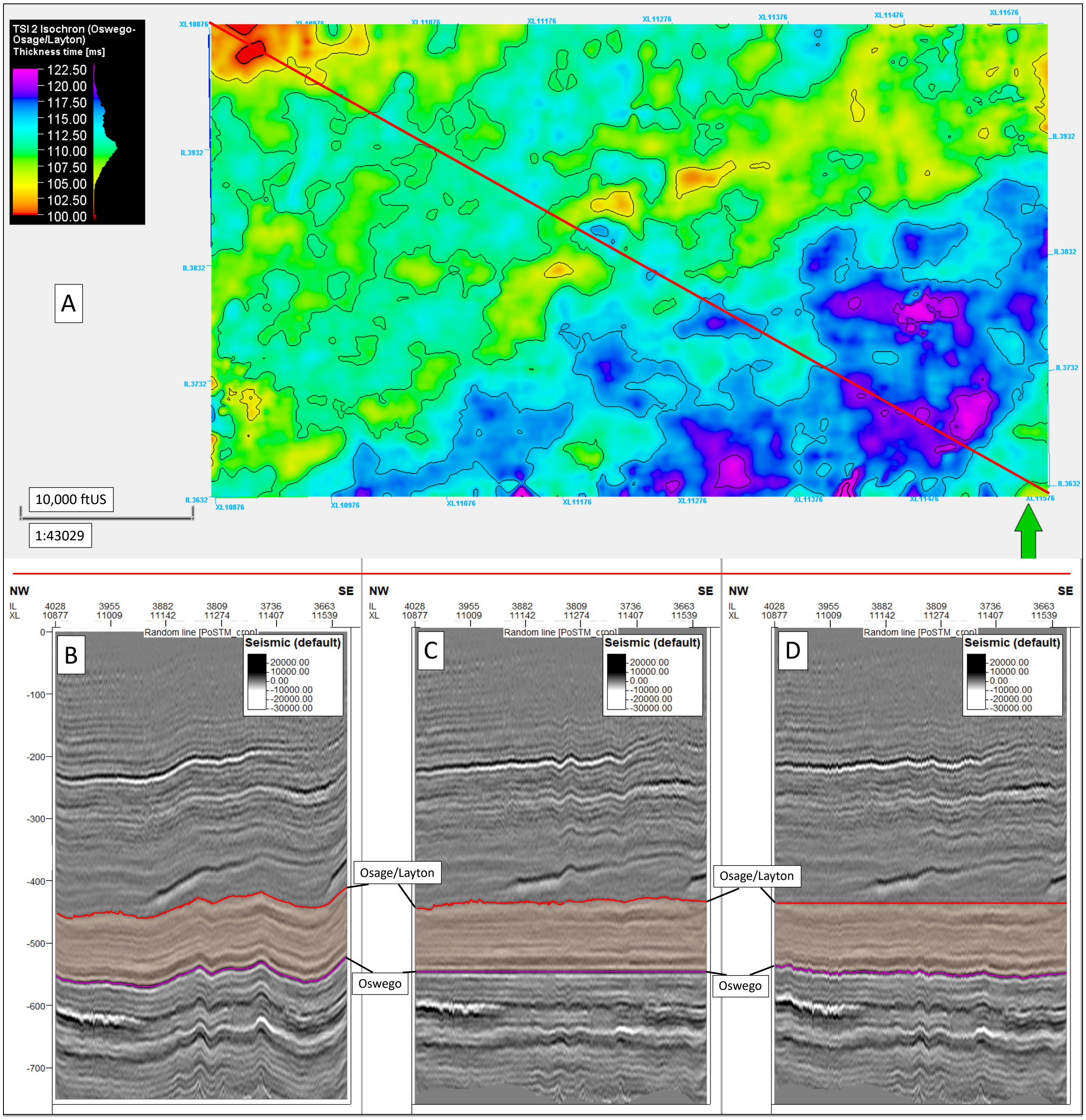

Figure 13: **A)** TSI2 isochron map; **B)** Seismic profile from WC showing the unflattened horizons of TSI-2 with the isochron interval exhibited on the map in "A" highlighted; **C)** Seismic profile from WC showing the flattened basal horizon (Oswego) with the isochron interval (Oswego-Osage/Layton) exhibited on the map in "A" highlighted; **D)** Seismic profile from WC showing the flattened upper horizon of TSI-2 (Osage/Layton) with the isochron interval (Oswego-Osage/Layton) exhibited on the map in "A" highlighted.

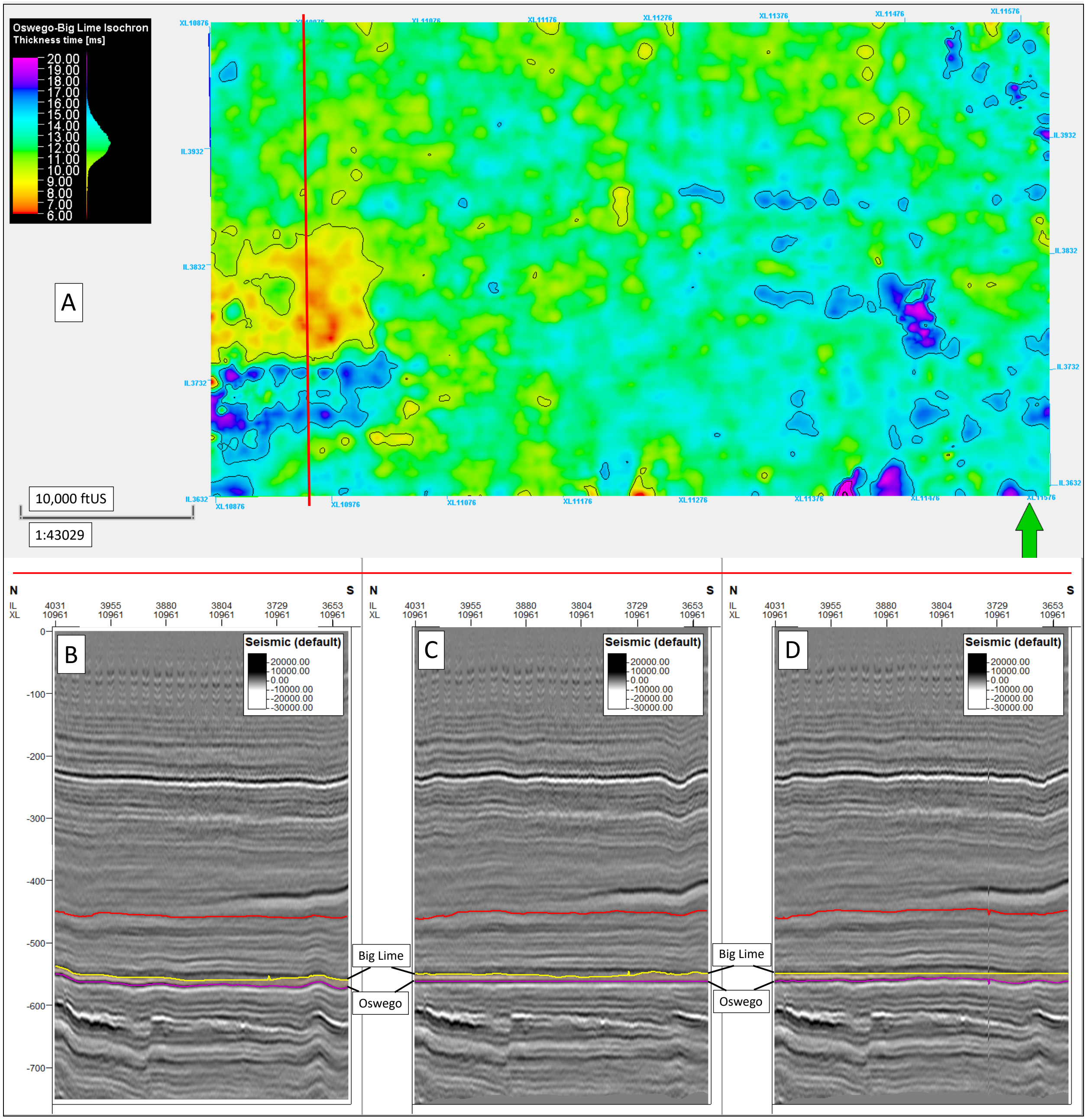

Figure 14: **A)** Oswego-Big Lime isochron map; **B)** Seismic profile from WC showing the unflattened horizons of the Oswego-Big Lime interval with the isochron interval exhibited on the map in "A" highlighted; **C)** Seismic profile from WC showing the flattened basal horizon (Oswego) with the isochron interval (Oswego-Big Lime) exhibited on the map in "A" highlighted; **D)** Seismic profile from WC showing the flattened upper horizon (Big Lime) with the isochron interval (Oswego-Big Lime) exhibited on the map in "A" highlighted.

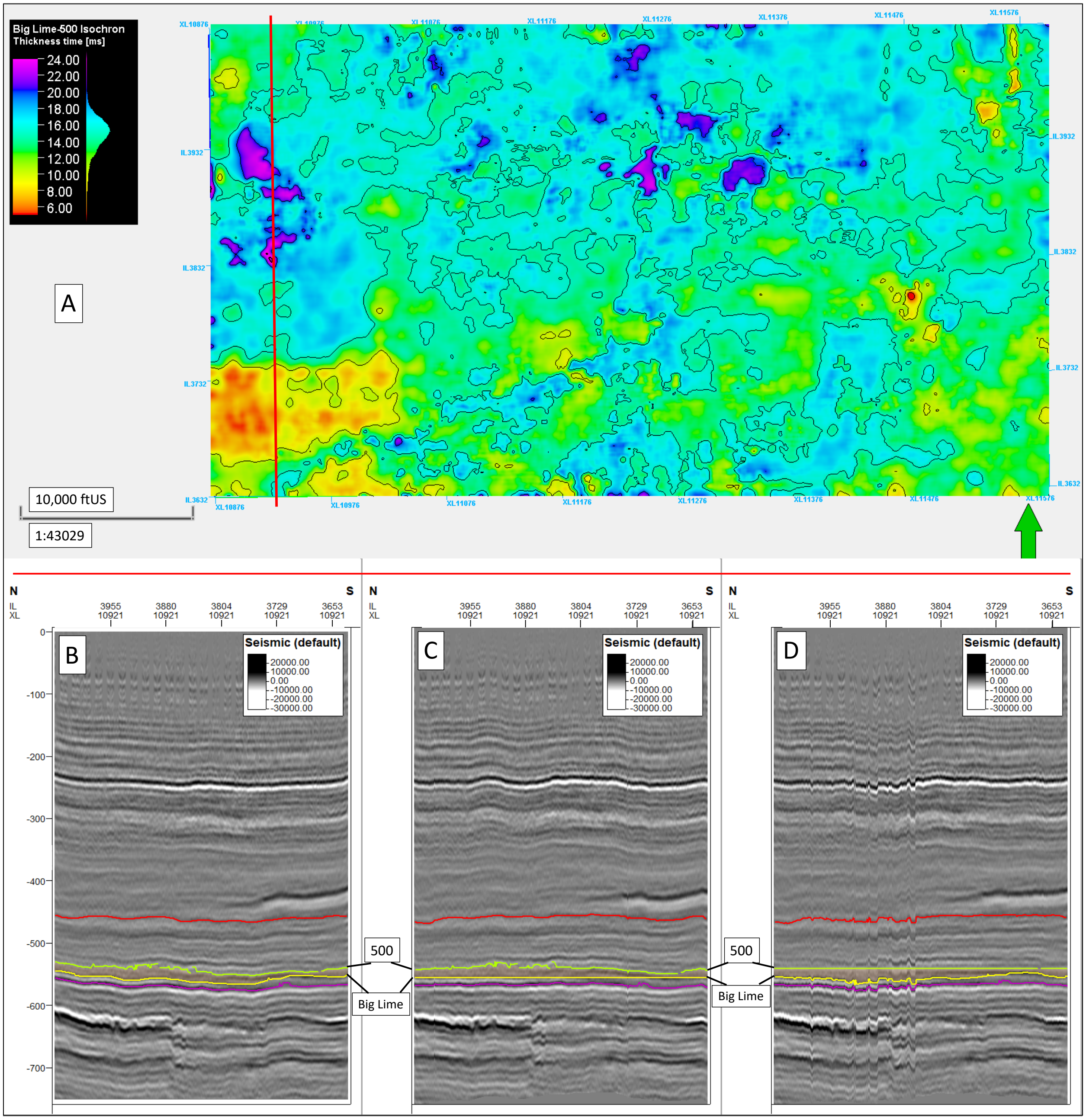

Figure 15: **A)** Big Lime-500 isochron map; **B)** Seismic profile from WC showing the unflattened horizons of the Big Lime-500 interval with the isochron interval exhibited on the map in "A" highlighted; **C)** Seismic profile from WC showing the flattened basal horizon (Big Lime) with the isochron interval (Big Lime-500) exhibited on the map in "A" highlighted; **D)** Seismic profile from WC showing the flattened upper horizon (500) with the isochron interval (Big Lime-500) exhibited on the map in "A" highlighted.

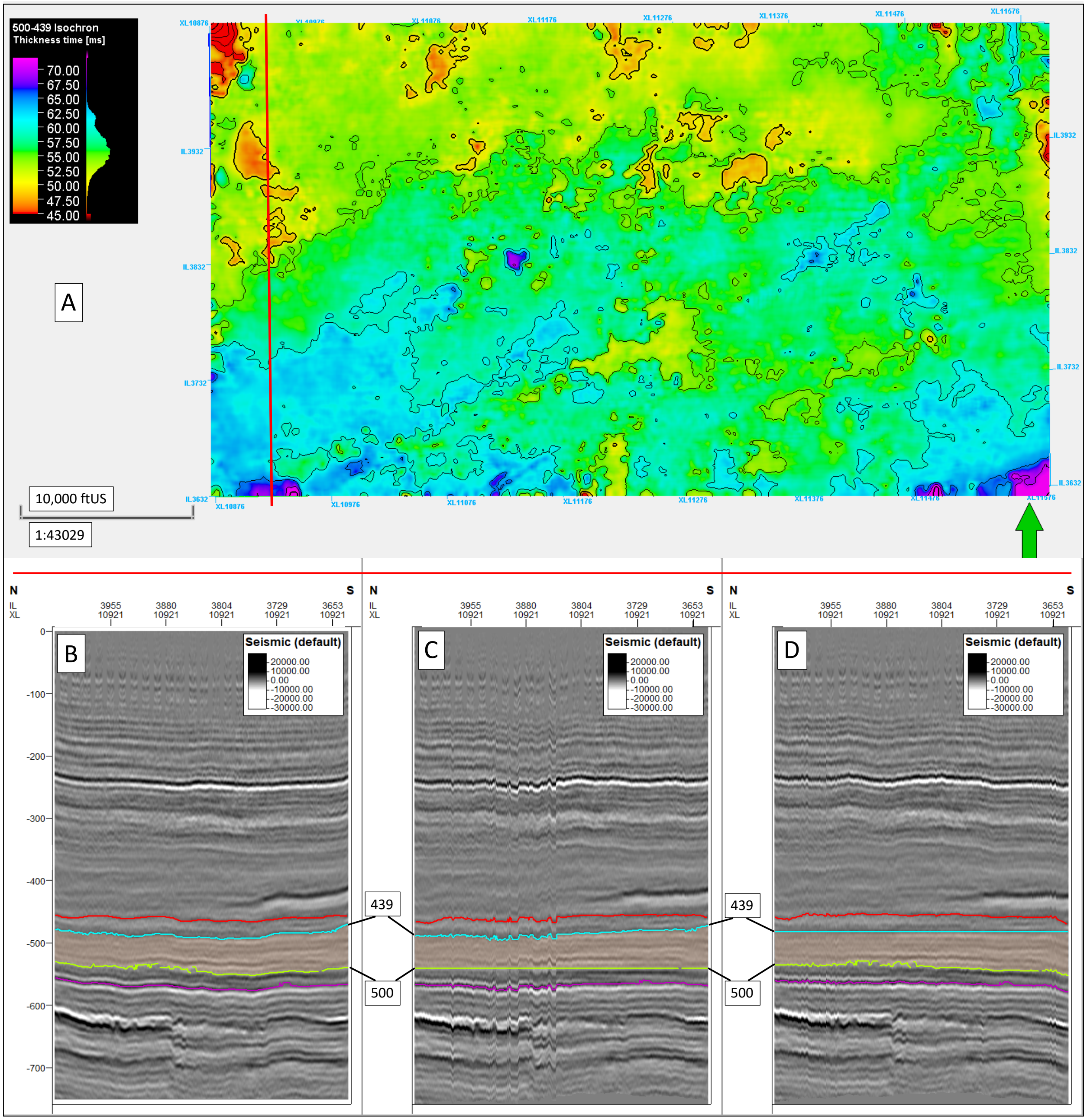

Figure 16: **A)** 500-439 isochron map; **B)** Seismic profile from WC showing the unflattened horizons of the 500-439 interval with the isochron interval exhibited on the map in "A" highlighted; **C)** Seismic profile from WC showing the flattened basal horizon (500) with the isochron interval (500-439) exhibited on the map in "A" highlighted; **D)** Seismic profile from WC showing the flattened upper horizon (439) with the isochron interval (500-439) exhibited on the map in "A" highlighted.

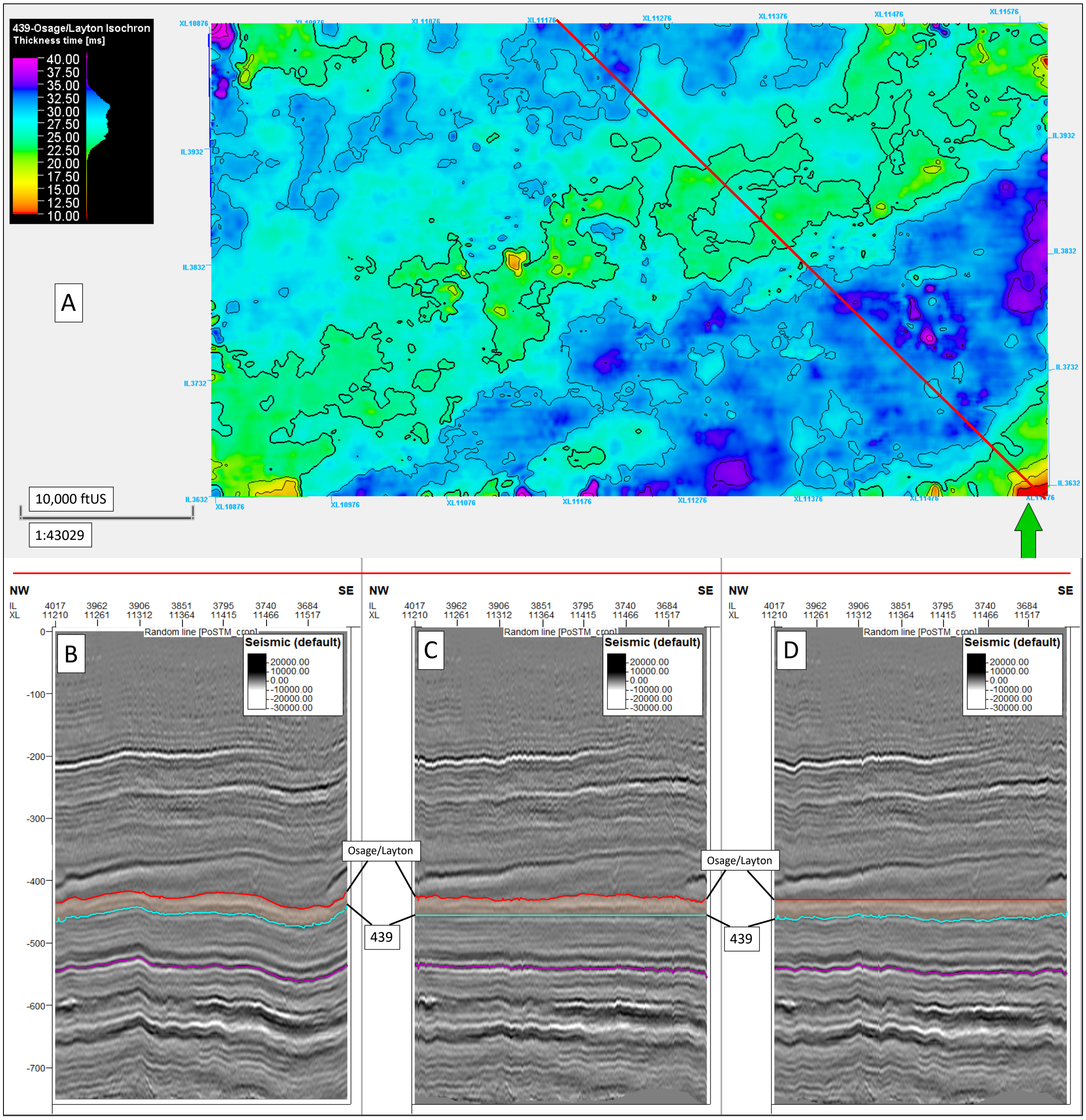

Figure 17: **A)** 439-Osage/Layton isochron map; **B)** Seismic profile from WC showing the unflattened horizons of 439-Osage/Layton with the isochron interval exhibited on the map in "A" highlighted; **C)** Seismic profile from WC showing the flattened basal horizon (439) with the isochron interval (439-Osage/Layton) exhibited on the map in "A" highlighted; **D)** Seismic profile from WC showing the flattened upper horizon (Osage/Layton) with the isochron interval (439-Osage/Layton) exhibited on the map in "A" highlighted.

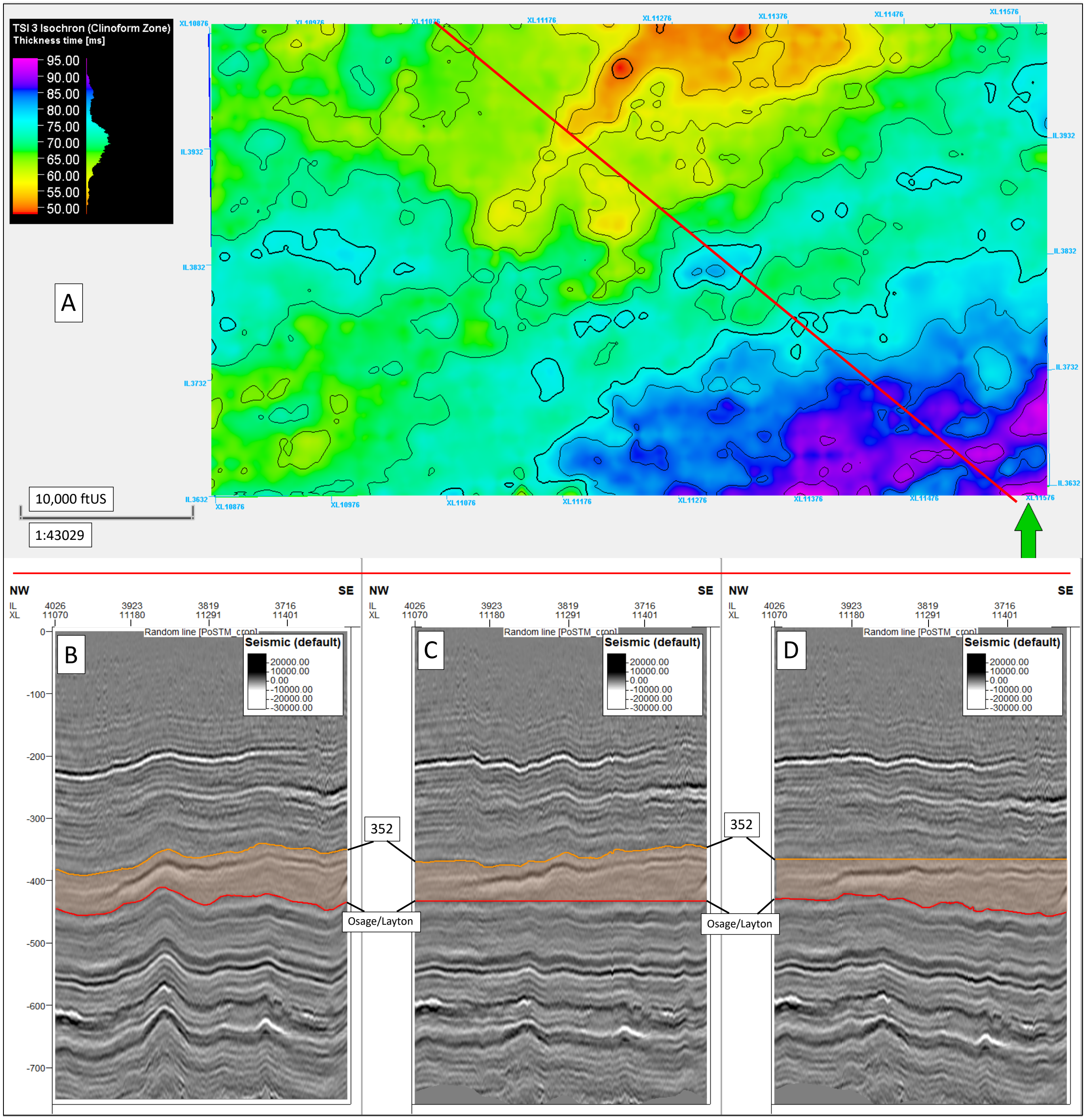

Figure 18: **A)** TSI-3 isochron map; **B)** Seismic profile from WC showing the unflattened horizons of TSI-3 with the isochron interval exhibited on the map in “A” highlighted; **C)** Seismic profile from WC showing the flattened basal horizon (Osage/Layton) with the isochron interval (Osage/Layton-352) exhibited on the map in “A” highlighted; **D)** Seismic profile from WC showing the flattened upper horizon (352) with the isochron interval (TSI-3) exhibited on the map in “A” highlighted.

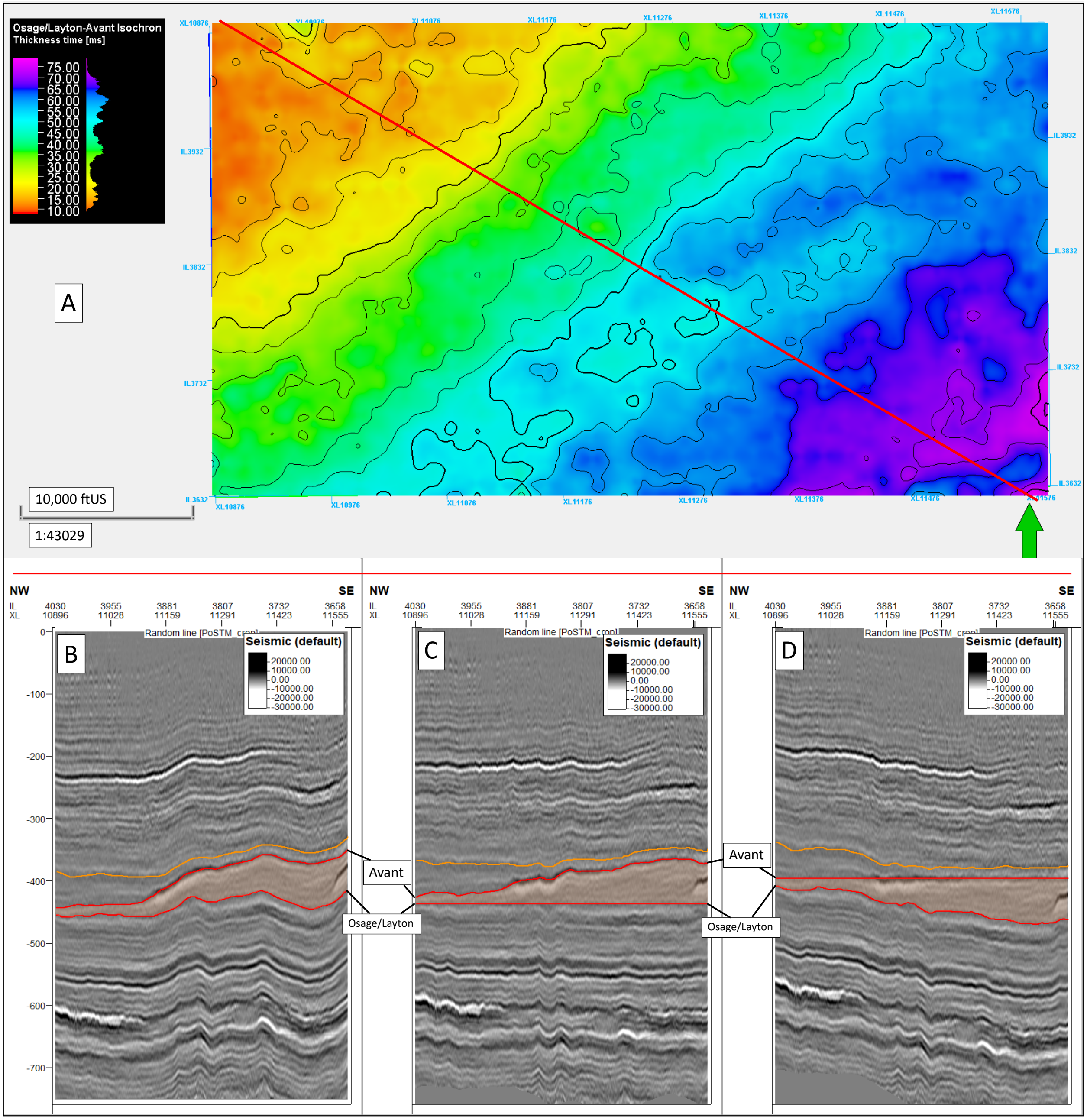

Figure 19: **A)** Osage/Layton-Avant isochron map with interpreted generalized normal fault trace overlain; **B)** Seismic profile from WC showing the unflattened horizons of Osage/Layton-Avant with the isochron interval exhibited on the map in "A" highlighted; **C)** Seismic profile from WC showing the flattened basal horizon (Layton/Osage) with the isochron interval (Avant-Layton/Osage) exhibited on the map in "A" highlighted; **D)** Seismic profile from WC showing the flattened upper horizon (Avant) with the isochron interval (Osage/Layton-Avant) exhibited on the map in "A" highlighted.

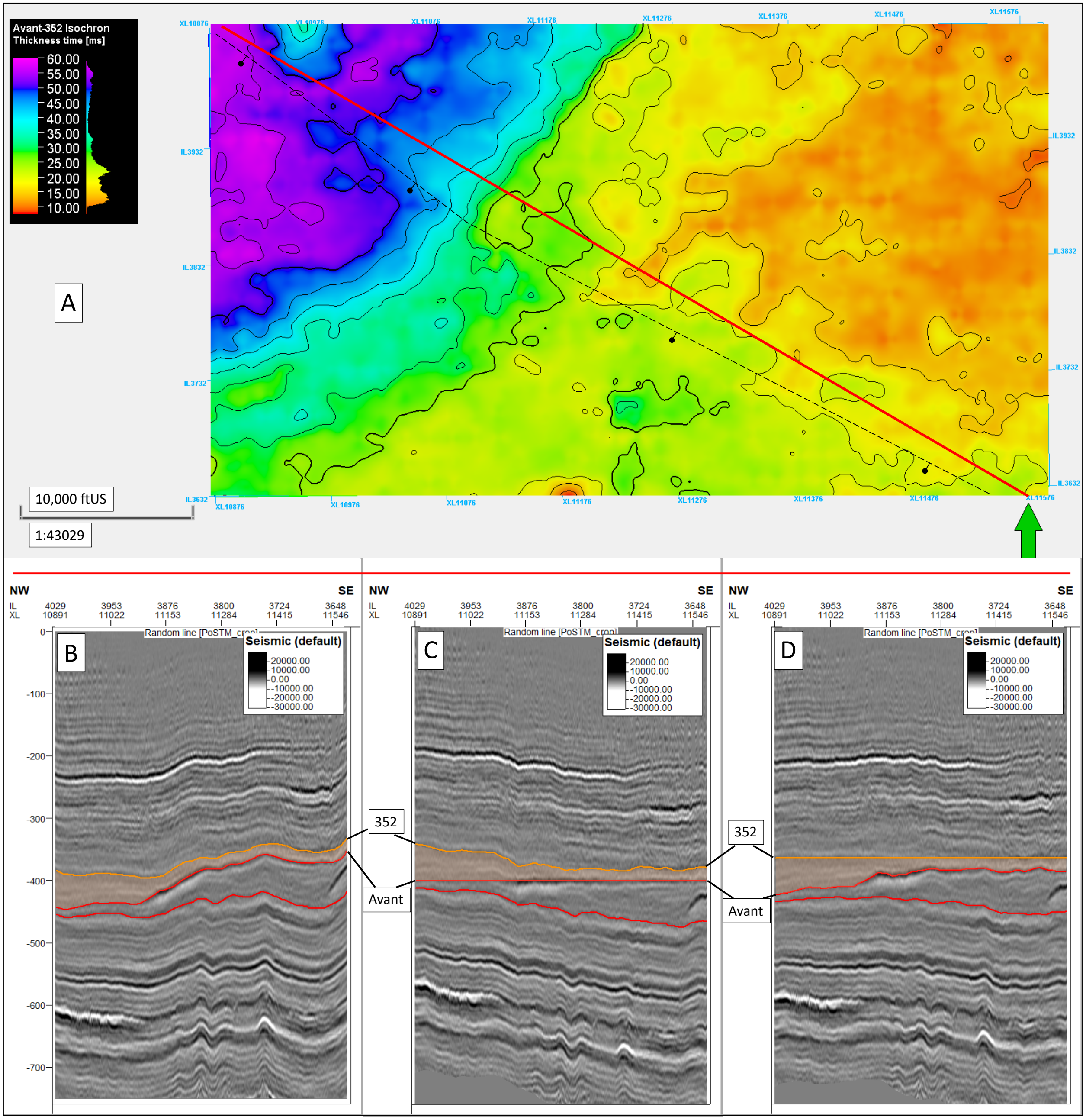

Figure 20: **A)** Avant-352 isochron with interpreted normal fault trace overlain; **B)** Seismic profile from WC showing the unflattened horizons of the Avant-352 interval with the isochron interval exhibited on the map in “A” highlighted; **C)** Seismic profile from WC showing the flattened basal horizon (Avant) with the isochron interval (Avant-352) exhibited on the map in “A” highlighted; **D)** Seismic profile from WC showing the flattened upper horizon (352) with the isochron interval (Avant-352) exhibited on the map in “A” highlighted.

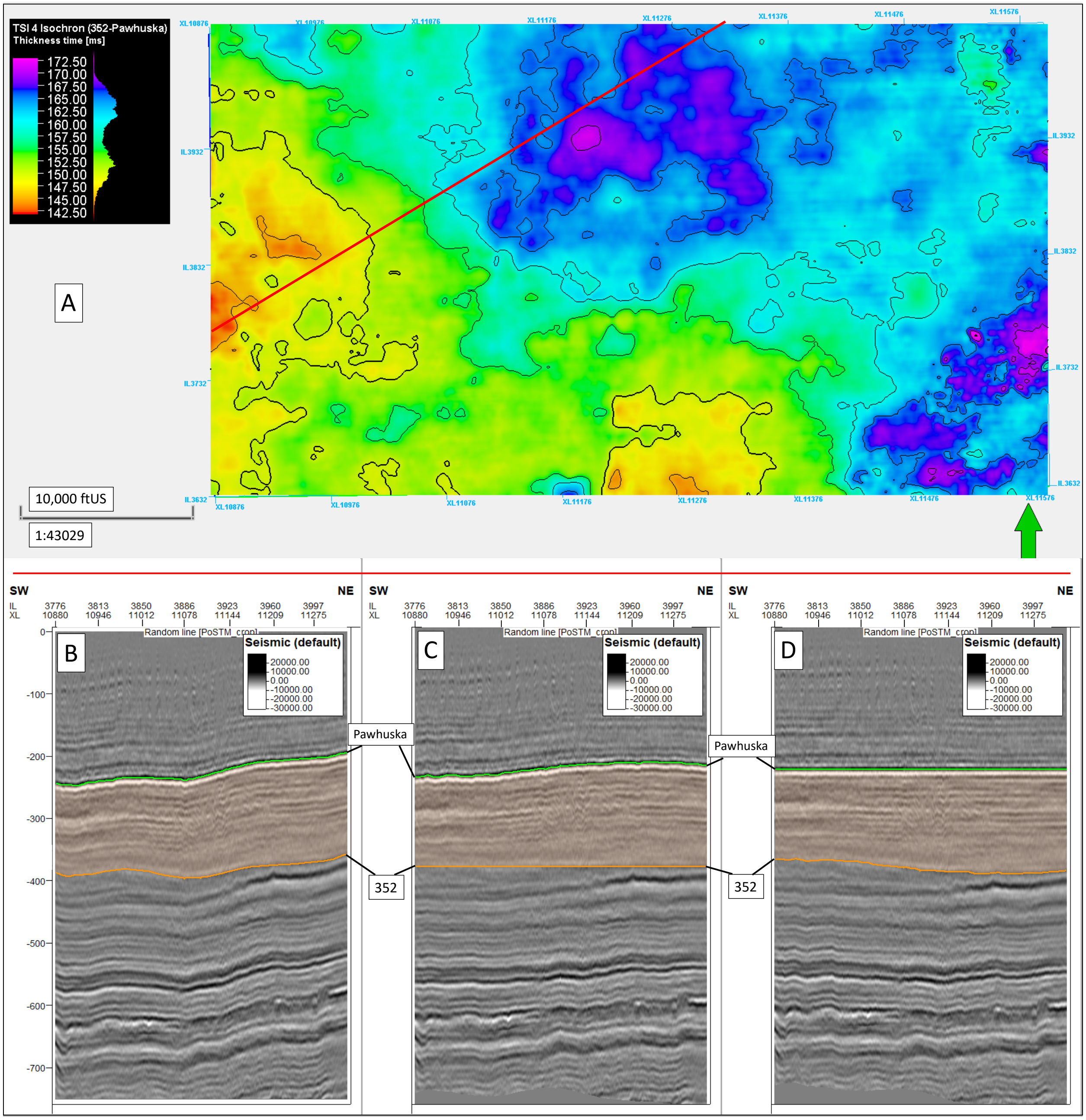

Figure 21: **A)** TSI-4 (352-Pawhuska) isochron map; **B)** Seismic profile from WC showing the unflattened horizons of TSI-4 with the isochron interval exhibited on the map in "A" highlighted; **C)** Seismic profile from WC showing the flattened basal horizon (352) with the isochron interval (352-Pawhuska) exhibited on the map in "A" highlighted; **D)** Seismic profile from WC showing the flattened upper horizon (Pawhuska) with the isochron interval (352-Pawhuska) exhibited on the map in "A" highlighted.

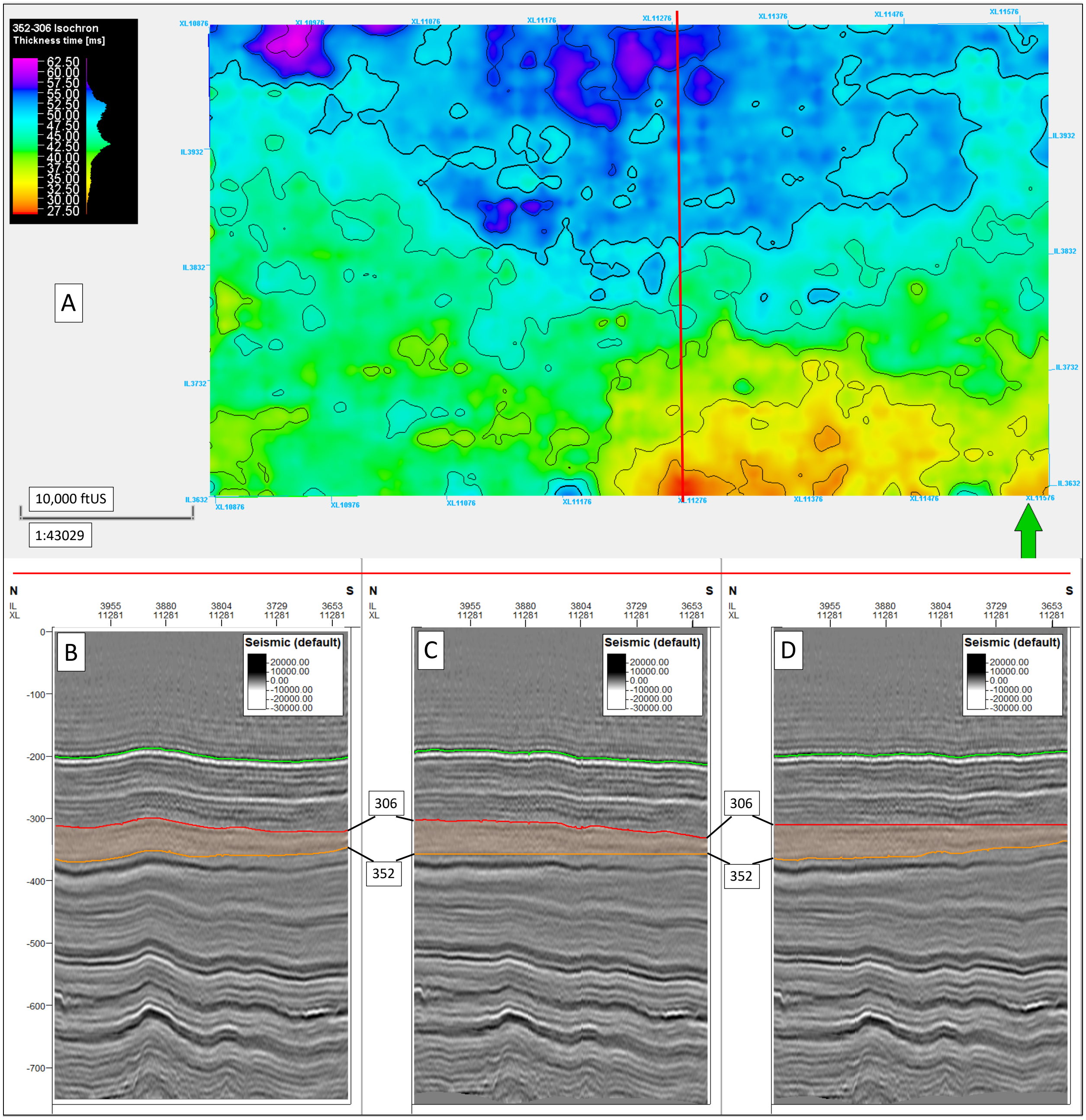

Figure 22: **A)** 352-306 isochron map; **B)** Seismic profile from WC showing the unflattened horizons of the 352-306 interval with the isochron interval exhibited on the map in "A" highlighted; **C)** Seismic profile from WC showing the flattened basal horizon (352) with the isochron interval (306-352) exhibited on the map in "A" highlighted; **D)** Seismic profile from WC showing the flattened upper horizon (306) with the isochron interval (352-306) exhibited on the map in "A" highlighted.

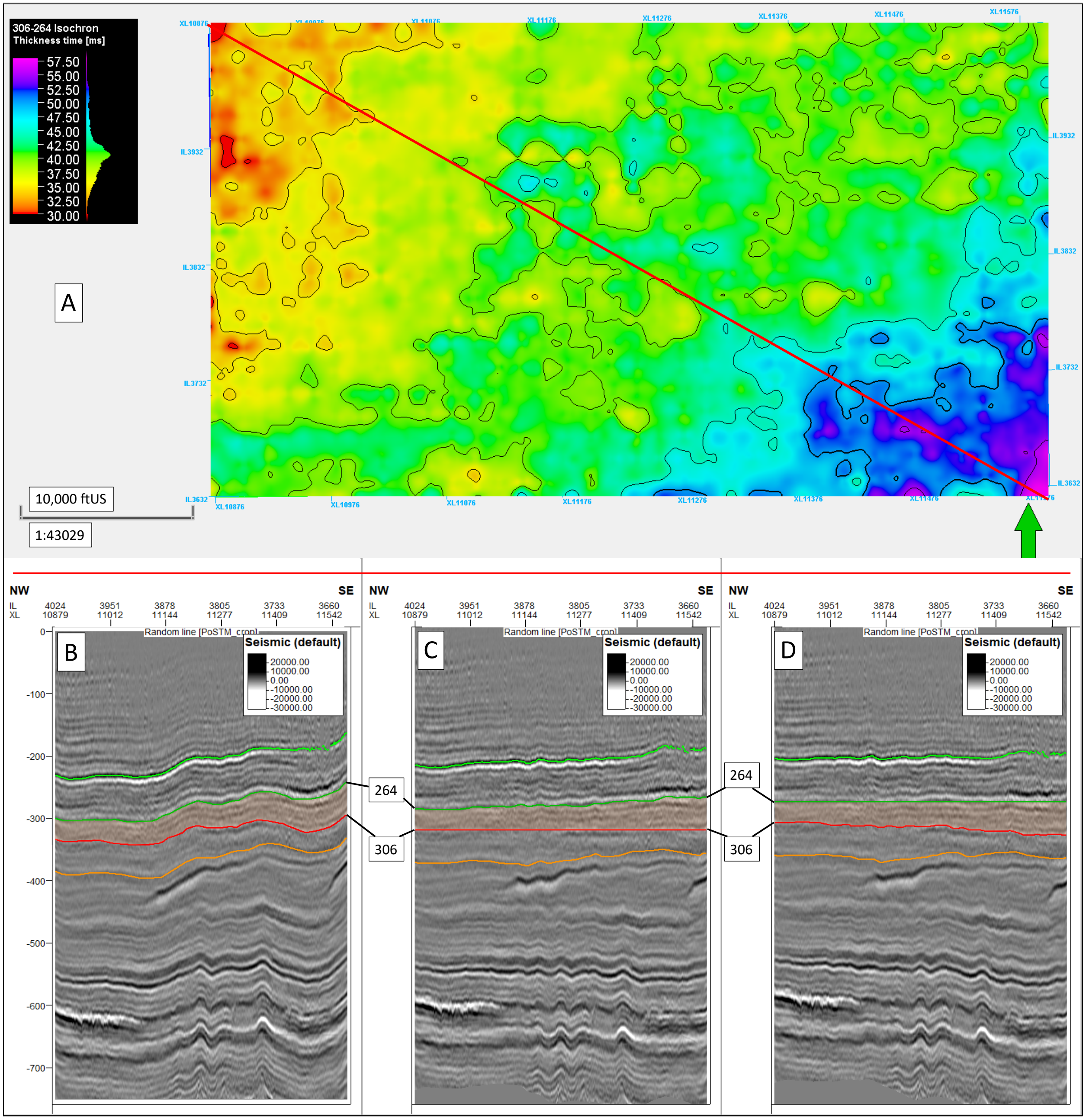

Figure 23: **A)** 306-264 isochron map; **B)** Seismic profile from WC showing the unflattened horizons of the 306-264 interval with the isochron interval exhibited on the map in "A" highlighted; **C)** Seismic profile from WC showing the flattened basal horizon (306) with the isochron interval (306-264) exhibited on the map in "A" highlighted; **D)** Seismic profile from WC showing the flattened upper horizon (264) with the isochron interval (306-264) exhibited on the map in "A" highlighted.

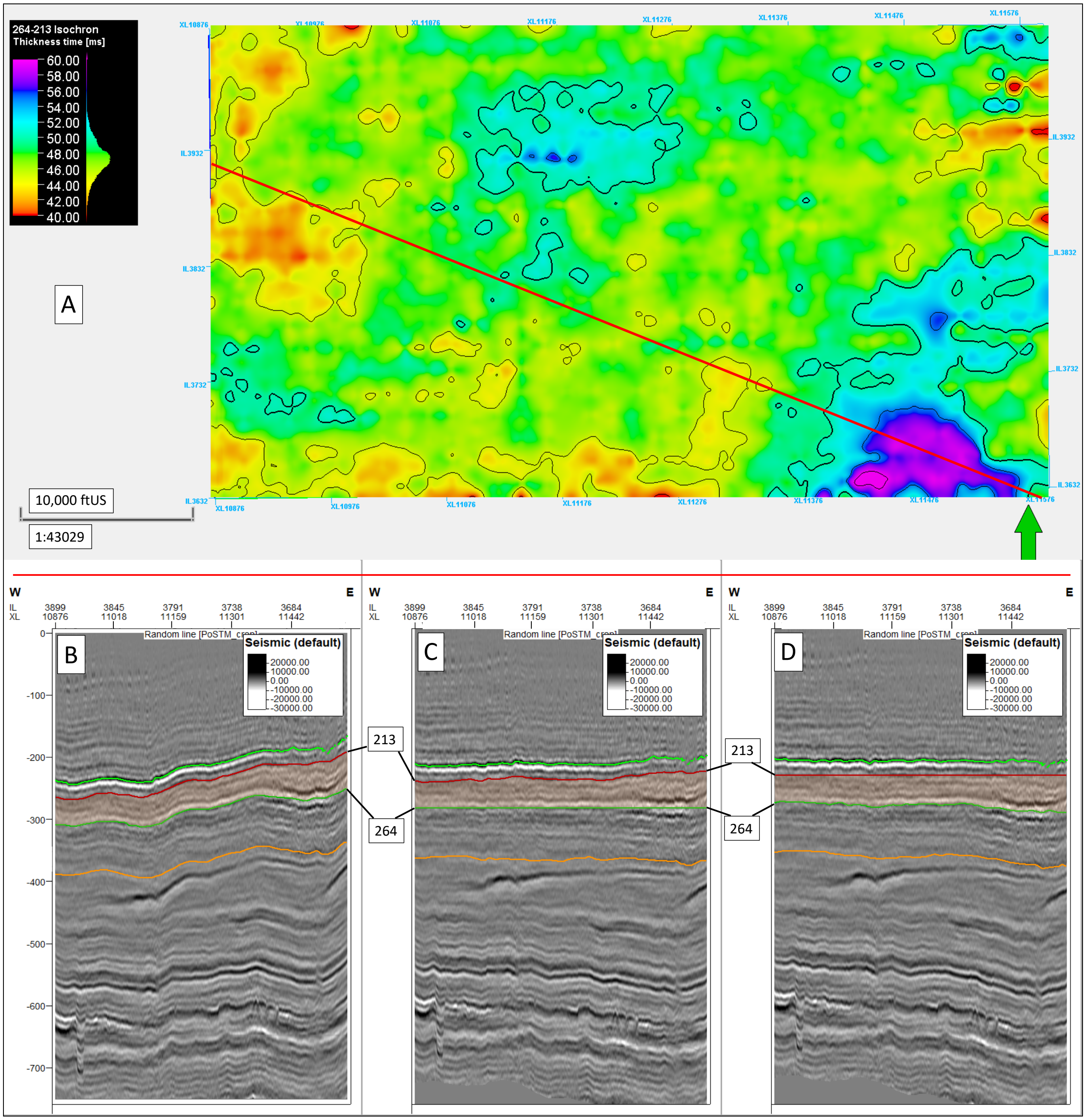

Figure 24: **A)** 264-213 isochron map; **B)** Seismic profile from WC showing the unflattened horizons of the 264-213 interval with the isochron interval exhibited on the map in "A" highlighted; **C)** Seismic profile from WC showing the flattened basal horizon (264) with the isochron interval (264-213) exhibited on the map in "A" highlighted; **D)** Seismic profile from WC showing the flattened upper horizon (213) with the isochron interval (264-213) exhibited on the map in "A" highlighted.

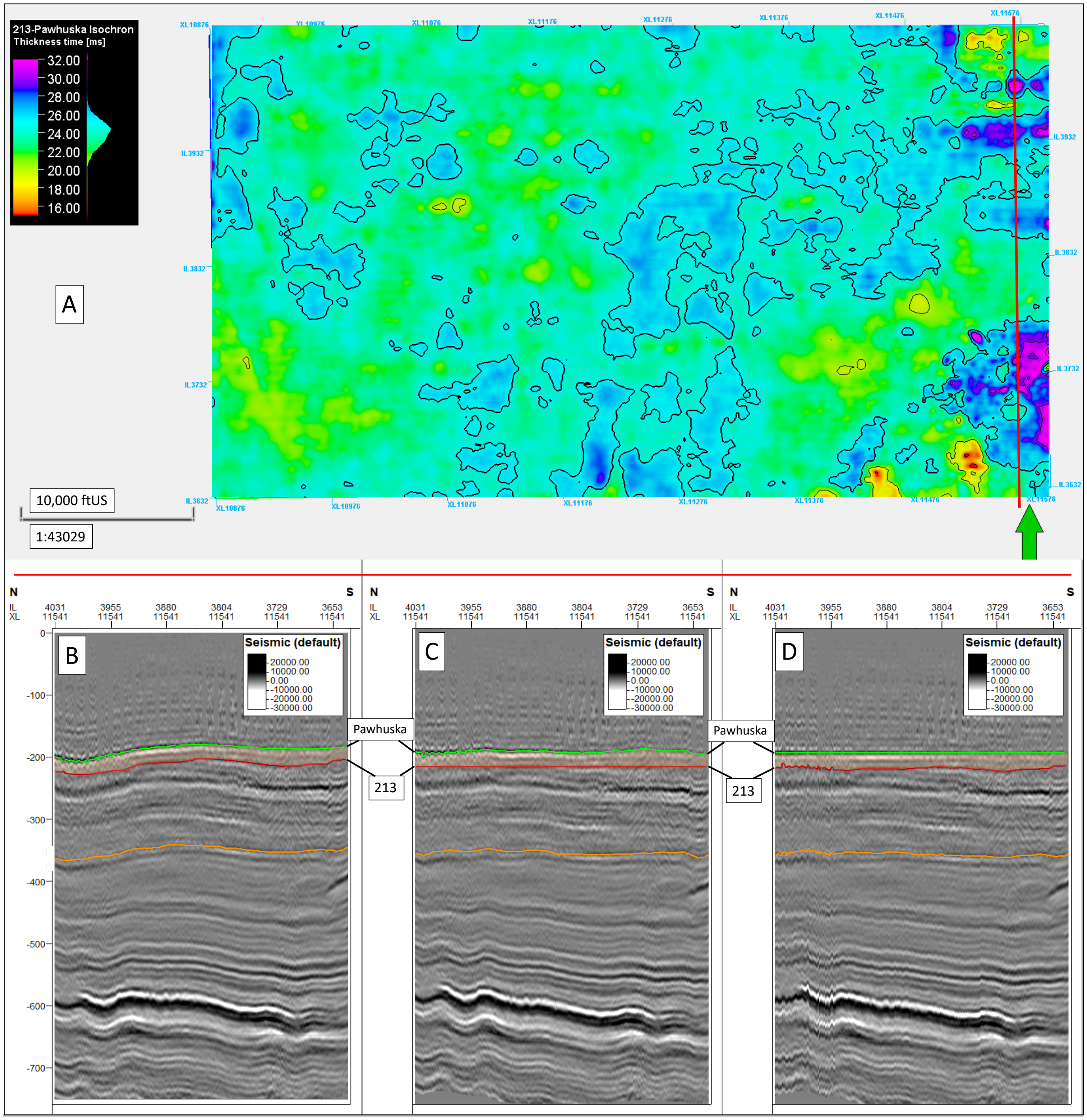

Figure 25: **A)** 213-Pawhuska isochron map; **B)** Seismic profile from WC showing the unflattened horizons of the 213-Pawhuska interval with the isochron interval exhibited on the map in "A" highlighted; **C)** Seismic profile from WC showing the flattened basal horizon (213) with the isochron interval (Pawhuska-213) exhibited on the map in "A" highlighted; **D)** Seismic profile from WC showing the flattened upper horizon (Pawhuska) with the isochron interval (213-Pawhuska) exhibited on the map in "A" highlighted.